
CHAPTER 2

LITERATURE REVIEW

2.1 Introduction

In this section, an overview of the operations at AngloGold Ashanti's No 2 Gold Plant operation is given. This is followed by a review of the mineralogy of the ore, collectors and activators used in this investigation. The thermodynamics of collector adsorption and mathematical models used to describe the kinetics of flotation are examined as well.

2.2 Operations at No. 2 Gold Plant – An Overview

The feed to the plant originates from two sources:

- Tailings from No. 2 Pumpcell Plant, which leaches reclaimed West Pay Dam material. Slimes are sluiced using a hydraulic gun. The resulting pulp is treated with lime and cyanide, and leached while being transported in an 11km pipeline. At the plant, it is stripped of any dissolved gold by contacting with carbon in a Carbon-In-Leach (CIL) circuit.
- Gold leached material from No. 9 Gold Plant, which is fed with run-of-mine ore from No. 9 Shaft at Tau Lekoa Mine.

The two tailings streams are combined and de-slimes using cluster cyclones. The mineralogy of the composite feed varies but a typical analysis derived from Figure 2.1 is shown in Table 2.1.

CHAPTER 2. LITERATURE REVIEW

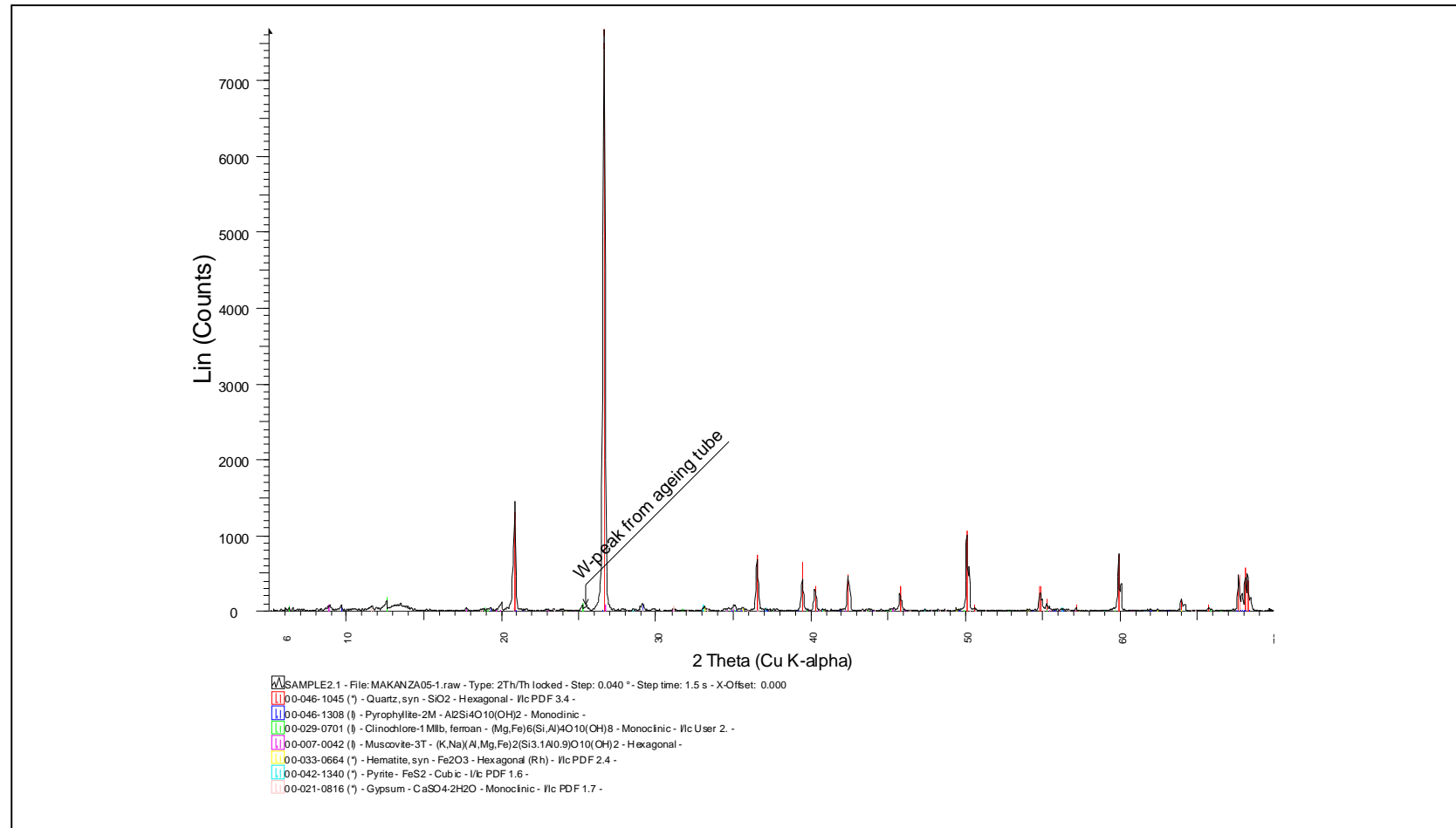


Figure 2.1 An XRD pattern for typical No. 2 Gold Plant feed

The main features are:

- Pyrite occurs in cubic form and can be either coarse or fine grained.
- Pyrophyllite is a naturally floatable clay mineral that comes from freshly mined material at No. 9 Shaft (Tau Lekoa Mine). It is removed from the feed by de-sliming.

Table 2.1 Typical minerals found in No. 2 Gold Plant Feed

Mineral	Chemical Formula
Quartz	SiO ₂
Pyrophyllite	Al ₂ Si ₄ O ₁₀ (OH) ₂
Clinocllore	(Mg,Fe) ₆ (Si,Al) ₄ O ₁₀ (OH) ₈
Muscovite	(K,Na)(Al,Mg,Fe) ₂ (Si _{3.1} Al _{0.9})O ₁₀ (OH) ₂
Hematite	Fe ₂ O ₃
Pyrite (cubic)	FeS ₂
Gypsum	CaSO ₄ .2H ₂ O

The overflow from de-sliming cyclones is sent to the Back-fill Plant while the underflow is conditioned with copper sulphate at a pH of 9.5 for about 10 hours. Thereafter, it is pumped to the float stock tank where it is reacted with an SO₂ containing solution called calcine water (Table 2.2) from the acid plant and additional copper sulphate.

Table 2.2 Chemical composition of calcine water (Dumisa, 2002)

Component	Pb	S	Fe	Al	Cu	Ni	Ca	Mg	Zn	U	SO ₄
Concentration (mg l ⁻¹)	2.5	1000	130	31	18	3.2	400	83	50	1.75	3410

At the end of the treatment, pulp pH is about 7.2. Mine water is added to achieve a final pulp specific gravity of 1.3. The pulp is divided into two streams. Each is treated with flotation reagents before being fed to flotation cells (Figure 2.2). Typical reagent dosages are shown in Table 2.3. The flotation circuit contains four rougher and two cleaner banks, which consist of eighteen and twelve cells in series respectively.

Table 2.3 *Typical reagent suite used at No. 2 Gold Plant (Dumisa, 2002)*

Reagent	Function	Dosage (g/t)
Copper Sulphate	Activator	70
SIBX	Collector	16
Dow200	Frother	16
GEMPOLYM GM4	Depressant	20

Concentrates collected from the first fourteen rougher cells are sent to the cleaner circuit while those from the last four are recycled to the float stock tank. The feed to the latter is treated with additional collector. All rougher tails are sent to the Back-fill Plant. In the cleaner bank, depressant is dosed into the first flotation cell. Concentrates collected from the first six cells (typically 28% sulphur) are thickened and sent to the acid plant while those from the last six are recycled to the cleaner bank's feed box. All cleaner tailings are recycled to the float stock tank (Dumisa, 2002).

CHAPTER 2. LITERATURE REVIEW

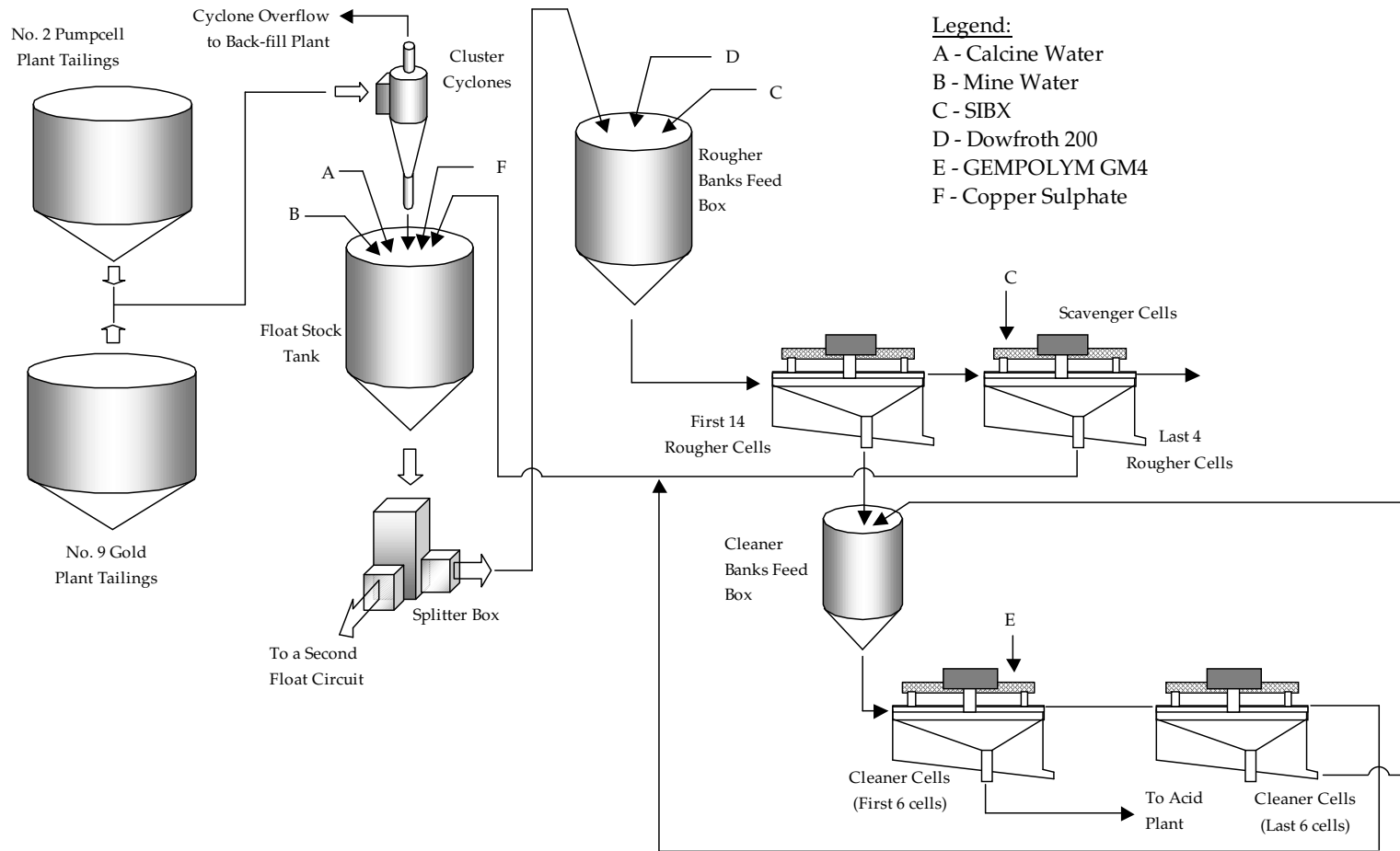


Figure 2.2 Flow sheet of the flotation circuit at AngloGold Ashanti's No. 2 Gold Plant (Dumisa, 2002)

2.3. Mineralogy of No. 2 Gold Plant Feed

2.3.1 Introduction

No. 2 Plant feed consists of reclaimed material from West Pay Dam and leach tails from No 9 Gold Plant (Dumisa, 2002). The latter treats ore received from Tau Lekoa and Kopanang Mines in separate streams. The two mining operations are exploiting the Ventersdorp Contact Reef and the Vaal Reef respectively (Browne, 2002). This section provides an overview of the geology of the latter. The focus is on mineralogy because of the significant impact it has on the flotation behaviour of the ore.

2.3.2 Mineralogy of the Vaal Reef

Like the rest of the Witwatersrand basin hosting it, the Vaal Reef is believed to originate from the Archaean granite-greenstone terrains that surround it (Anhaeusser et al., 1987). Its sediments range from coarse conglomerates to coarse arenites. Cemented by a fine-grained matrix of re-crystallised quartz and phyllosilicates^ψ, the former predominate. They are greyish metamorphosed sedimentary rocks that consist of mainly muffin-shaped pebbles of quartz ($\approx 80\%$ by mass) (Figure 2.3). The pebbles vary in composition, size and colour. The larger ones of vein quartz averaging about 40 to 50mm predominate and are sometimes accompanied by pebbles of other materials such as quartzite, chert, red jasper, and quartz porphyry (Robb and Meyer, 1995). Except for occasional veinlets and inclusions of sulphides and rare gold, the pebbles are barren. The matrix (Table 2.4) invariably contains visible pyrite, accompanied by other sulphides such as pentlandite, pyrrhotite, galena, sphalerite and chalcopyrite in diminutive amounts. Visible gold is rare (Ford, 1993).

^ψ A mixture of muscovite and chlorite and sometimes pyrophyllite and/or chloritoid

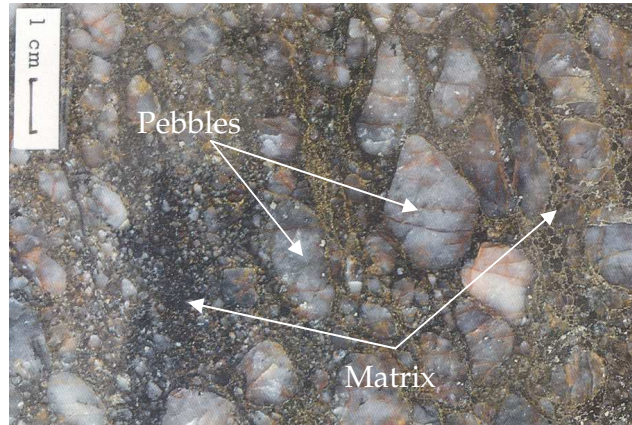


Figure 2.3 Conglomerate comprised of pebbles of quartz embedded in an essentially quartz rich matrix. Grain boundaries are outlined by phyllosilicates and fractures by recent oxidation of pyrite to iron oxides. Macrophotograph, linear magnification $\times 0.6$ (after Anhaeusser et al., 1987)

Table 2.4 Vaal Reef pebble cementing matrix (Ford, 1993)

Major Constituents		Minor Constituents		Rare Constituents	
Pyrite		Arsenopyrite Cobaltite Gersdorffite	Sulpharsenides	Gold	
Rutile Leucoxene	As separate or composite grains	Pyrrhotite Sphalerite Galena Chalcopyrite	Sulphides	Platinum Group Minerals	
Chromite		Anatase U-bearing minerals		Marcasite Pentlandite Mackinawite Millerite	Sulphides
Zircon		Chloritoid		Tucekite	
Sericite Pyrophyllite Chlorite	Phyllosilicates			Illite Kaolinite	Phyllosilicates
				Tormaline	
				Churchite Xenotime	Yttrium Phosphates
				Apatite	

The reef is characterised by the presence of discontinuous patches of carbonaceous matter, intimately associated with uraninite and gold. Occasionally, the uraninite is found in the form of round compact grains, enveloped and/or partially replaced by the carbonaceous matter (also called karogen). The latter has been sometimes referred to as bitumen since it is

largely regarded as organic material that was once a mobile viscous liquid and has since solidified (Simpson and Bowels, 1977). During sedimentation, the enveloped uraninite must have escaped oxidation but not dissolution. This conclusion is drawn from some grains found in the matrix. Because of lack of protection, they formed a brannerite species, most probably through leaching of their uranium content by hydrothermal fluid. Based on their optical characteristics, two distinct species of the brannerite are recognised. One resembles leucoxene[§] and the other, brannerite of hydrothermal origin. The optical differences between the two varieties are linked to a compositional delimitation that can be expressed as a ratio between the oxides of uranium and those of titanium. The species with a ratio below 1 are referred to as uraniferous leucoxene and those above this value, brannerite.

Karogen may also occur as isolated round nodules within which an association with uranium is less obvious. Gold is very often intimately associated with such karogen seams both along the edges and within the hydrocarbon (Figure 2.4).

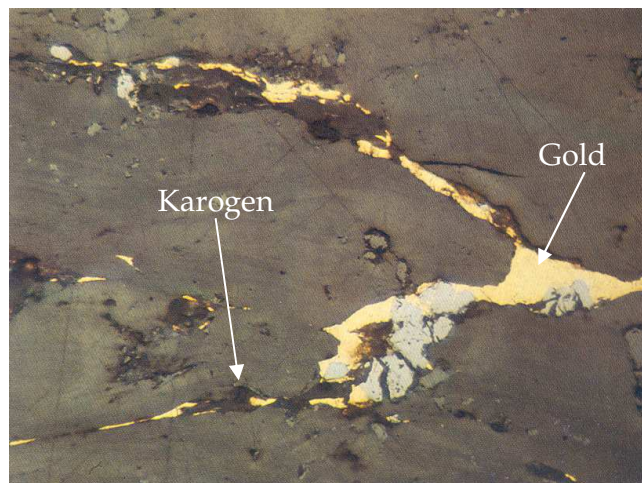


Figure 2.4 Photomicrograph showing uraniferous karogen containing inter- and intra-columnar gold, Carbon Leader Reef, Doornfontein Mine. Linear magnification $\times 135$ (Anhaeusser et al., 1987)

[§] The earthly variety of rutile

A distinction is made between detrital⁸ gold and that which was deposited, dissolved, transported and re-precipitated elsewhere (Robb and Meyer, 1995). Due to exclusion during crystallisation, the latter is found at pyrite grain boundaries. Consequently, the association existing between pyrite and the metals uranium (in the form of uraninite) and gold is of a purely sedimentological nature. Concentrations of pyrite do not always carry uraninite and/or gold. Their presence depends chiefly on the supply from the source rock at the time of sedimentation in addition to post-depositional reactions. The other sulphides *viz.* (pyrrhotite, sphalerite, galena, chalcopyrite, marcasite and pentlandite) were all precipitated after the detritus had been deposited. The following uranium-bearing minerals (all containing tetravalent uranium) contribute to the mineralisation in the reef:

Uraninite	UO ₂ , enclosed in the matrix or by karogen
Brannerite type minerals	U _{1-x} Ti _{2+x} O ₆
Coffinite	(U,Th)SiO ₄
Uraniferous Zircon	ZrSiO ₄

The uranium content of the uraniferous zircon is negligible and coffinite is rare. The most important carriers of uranium are primary uraninite and minerals of the brannerite type. The former may contain minute specks of up to 20% by mass of galena per grain (Ford, 1993). This is thought to have formed from lead, a product of the radioactive decay of uranium. An example involving the U²³⁸ isotope is shown in Figure 2.5.

⁸ Transportation of discrete grains from their place of origin, followed by deposition

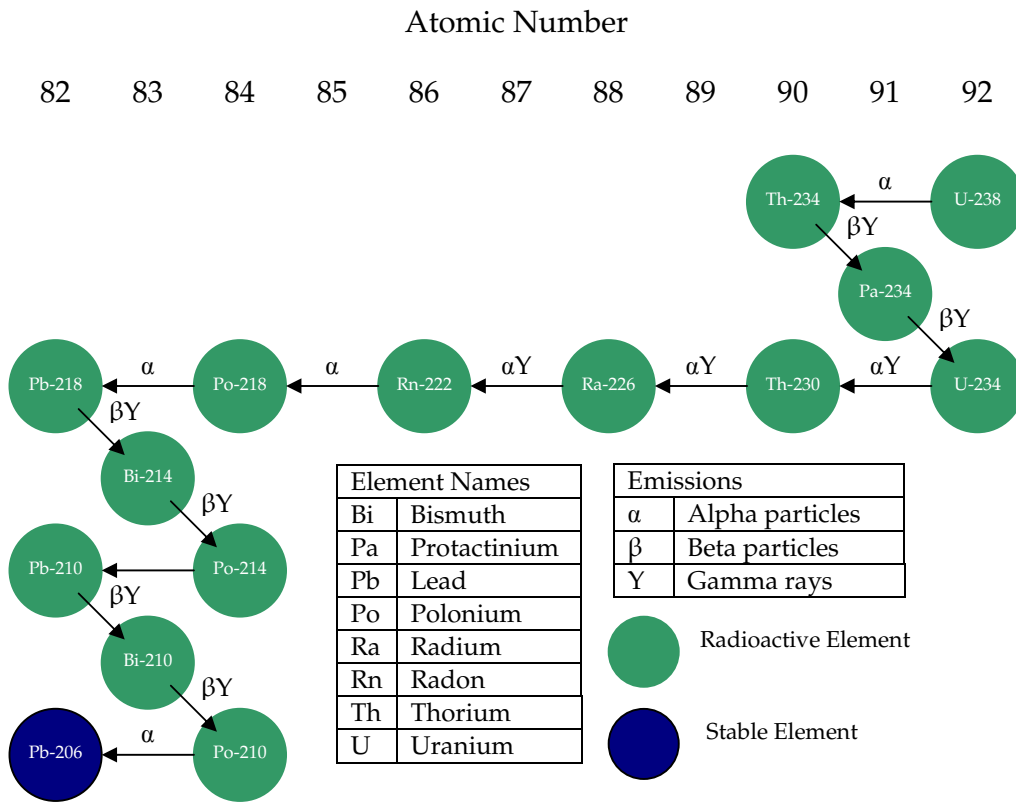


Figure 2.5 The radioactive decay of U^{238} to Pb^{206} (The Nuclear History Site, 2002)

2.4. Fundamentals of Froth Flotation

2.4.1 An Overview of the Flotation Process

Froth flotation is a beneficiation process that utilises the differences in physico-chemical surface properties of minerals, finely divided and suspended in an aqueous medium to effect separation. It involves the attachment of air bubbles to mineral particles that have been selectively rendered hydrophobic. The aggregates formed then rise to the surface where they form a metastable froth phase (Crozier, 1992). Ores generally consist of valuable mineral particles that are intimately associated with gangue. After milling and liberation of mineral values and adjustment of pulp density, various chemical constituents are added to modify constituent minerals. For effective collection of valuables from gangue, a concentration process by froth flotation follows.

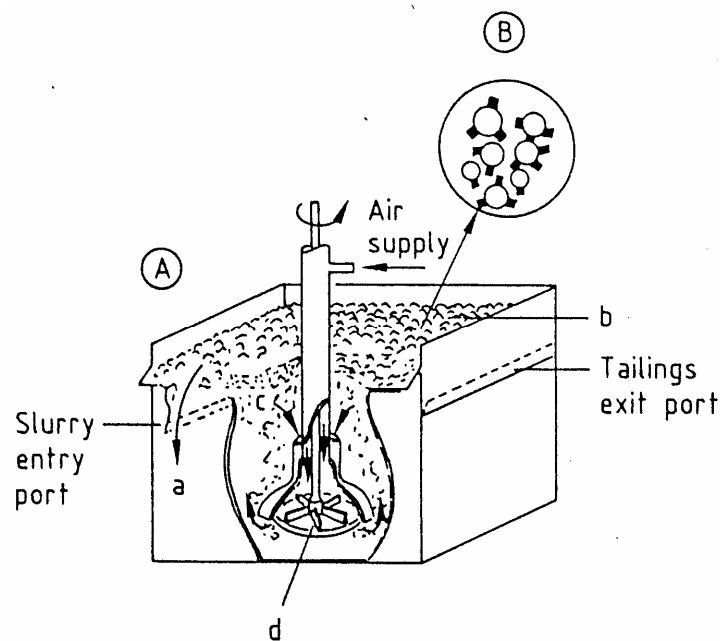


Figure 2.6 Processes occurring in a flotation cell (A) Flotation cell a) Froth overflow; b) Froth layer; c) Pulp; d) Rotor for pulp agitation; (B) Mineralised air bubbles within flotation cell (Yarar, 1985).

Sulphydryl collectors have the role of selectively attaching to sulphide minerals and producing a water repellent film. A frother is used to impart an internal hydrophobic character to a bubble which after an effective collision with a coated valuable particle allows certain stability to mineral-laden air bubbles after they reach the surface. Depressants are added to exclude undesirable minerals called gangue from attaching to the air bubble by imparting a hydrophilic character to them.

2.4.2 Thermodynamic Considerations

Based on thermodynamic phase equilibrium, Davidtz (1999) proposed the use of activity coefficients to quantify the degree of hydrophobicity of surfaces coated with surfactant molecules. Under surface coverage conditions that do not exceed monolayer coverage, and where chain length and concentration of collector molecules were below the critical micelle concentration, it was possible to quantify the thermodynamic factors involved in the phase separation between water and a suspended particle.

The conclusion reached was that for a given particle size and temperature, only the amount (X_i) and type of collector functional groups reflected in the activity coefficients of interacting water and functional groups (γ_i) determined the degree of phase separation between a particle and water. Furthermore, the greater the degree of phase separation, as reflected by the Excess Gibbs Free Energy, the more readily the particle floated. Effectively, it was assumed that a freshly exposed surface would be hydrated and hydrophilic, and that progressively, this would become more hydrophobic as collector coverage increased. Eventually, a two-phase region is formed in which surface adsorbed collector molecules (phase α) are surrounded by water (phase β). (Figure 2.7 (b))

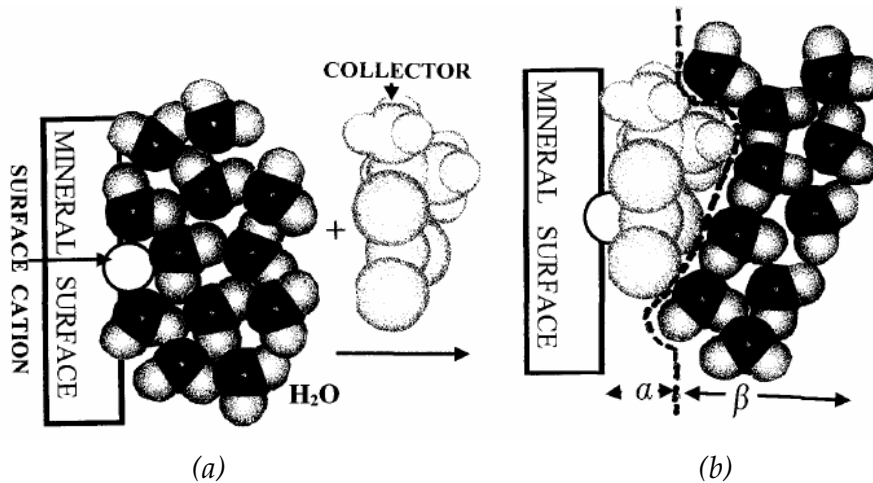


Figure 2.7 Zone where mineral surface-collector-water interactions take place (Davidtz, 1999)

The Excess Gibbs Free Energy (G^{ex}) is defined by:

$$G^{ex} = RT \sum x_i \ln \gamma_i \quad [2.1]$$

Where x_i = mole fraction

γ_i = activity coefficient for the i^{th} component

Support to the method was claimed by comparing G^{ex} values calculated with the UNIFAC method to experimental data from batch flotation tests using a copper ore at starvation reagent dosages. Time-recovery data obtained were used to determine cumulative recovery (R) and mean initial rate (K). Fitting a linear relationship between the calculated G^{ex} values and K gave R-squared values very close to 1, implying a strong correlation (Figure 2.8). Similarly, results from the flotation of a mixed sulphide ore containing chalcopyrite, galena, sphalerite, pyrrhotite with covalent TTC also showed a strong linear correlation between G^{ex} and fractional recovery (Figure 2.9). From these findings, Davidtz (1999) concluded that Gibbs excess free energy is directly

proportional to both initial rate and fractional recovery. In other words, for different collectors, G^{ex} can be used to predict flotation performance.

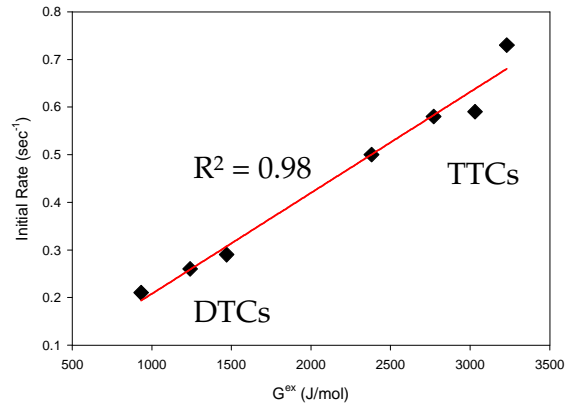


Figure 2.8 Initial rate- G^{ex} relationship for DTCs and TTCs on copper (Davidtz, 1999)

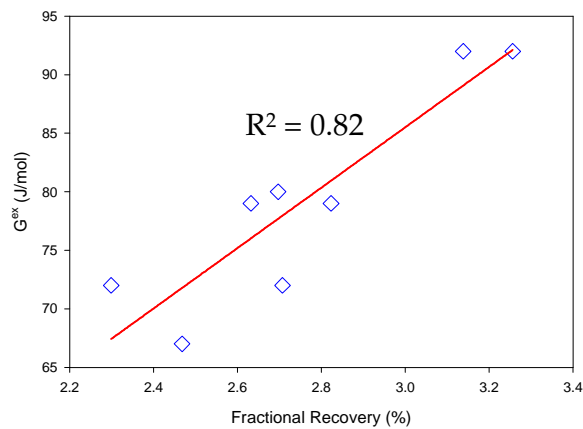


Figure 2.9 Relationship between G^{ex} and recovery for covalent TTC collector molecules (Davidtz, 1999)

Davidtz (2005) summarized the interacting variables as follows:

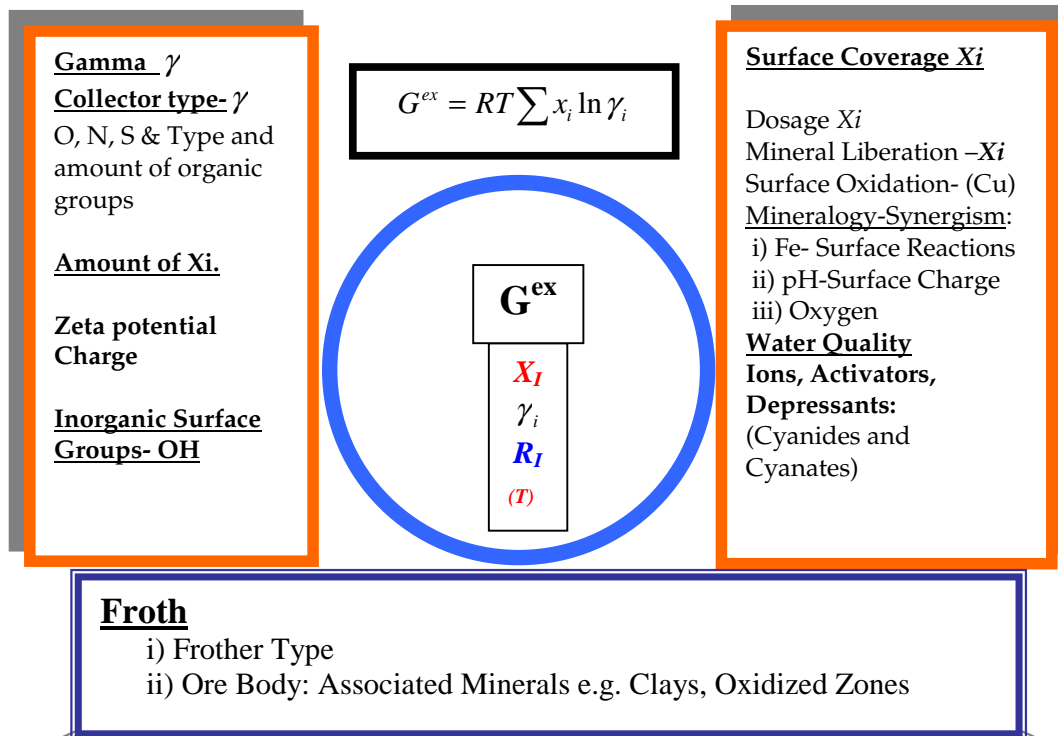


Figure 2.10 A summary of interacting variables in flotation (Davidtz, 2005)

2.4.3 Contact Angle

Particle-bubble attachment is known to occur when a solid surface is hydrophobic. The stability of the attachment is measured by the contact angle, θ (Figure 2.11) developed between the two phases: the air bubble (gas) and the surface of the mineral (solid). When an air bubble does not displace the aqueous phase, the contact angle is zero. On the other hand, complete displacement represents a contact angle of 180° . Values of contact angles between these two extremes provide an indication of the degree of surface polarity, or conversely, the hydrophobic character of the surface.

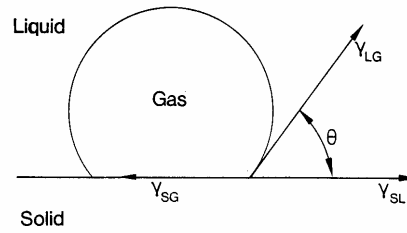


Figure 2.11 Schematic representation of the equilibrium contact between an air bubble and a solid immersed in a liquid (Fuerstenau and Raghavan, 1976)

The maximum free energy change per unit area, G^{ex} , corresponding to the attachment process (the displacement of the water by the air bubble) can be expressed by:

$$\Delta G = \pi_{SG} - (\pi_{SL} + \pi_{LG}) \quad [2.2]$$

Where π_{SG} , π_{SL} and π_{LG} are surface energies between the solid-gas, solid-liquid and liquid-gas phases respectively. Since the three-phase equilibrium existing in the system can be described in terms of the respective interfacial tensions according to:

$$\pi_{SG} = \pi_{SL} + \pi_{LG} \cos \theta \quad [2.3]$$

Where θ is the contact angle between the mineral surface and the air bubble, the free energy change can be expressed as:

$$\Delta G = \pi_{LG} (\cos \theta - 1) \quad [2.4]$$

Further support for Gibbs Excess Free Energy is in its relationship to contact angle and hence hydrophobicity: At constant temperature and composition, the change in G^{ex} is the product of the surface area and the change in surface tension, π .

$$dG^{ex} = Ad\pi \quad [2.5]$$

2.4.3 Flotation Rate

The flotation response of minerals at different experimental conditions has been traditionally studied through laboratory batch tests in which the recovery of the target mineral is measured at the end of a certain period of time. Klimpel (1980) drew attention to the loss of valuable information on the recovery kinetics as a drawback associated with this method. Instead, the author proposed the use of release curves. This approach is based on the fact that flotation is primarily a rate process that can be described by a first-order rate equation. Concentrates are collected over preset time intervals. The recovery-time data obtained are fitted into a model that describes recovery as a function of time. According to Klimpel (1984a), using models makes it is easier to compare and statistically test differences between recovery-time profiles by studying their model parameters instead of actually testing the profiles themselves. The more the conditions tested, the more the profiles involved, and the more difficult it will be to recognise trends and test significant differences using profiles only. The author also emphasised that the most suitable models are those that have two curve-fitting parameters. Since optimal parameters from curve fitting have broad confidence ranges, models having more than two curve-fitting parameters result in over-fitting of data, making the parameters lose their physical meaning.

Slabbert (1985) listed various equations that have been developed for describing the flotation process:

$$\text{Klimpel's Equation:} \quad R = R_{\max} \left(1 - \frac{1}{Kt} (1 - e^{-kt}) \right) \quad [2.6]$$

$$\text{Gamma Equation:} \quad R = R_{\max} \left(1 - \frac{\gamma}{(\gamma + t)^p} \right) \quad [2.7]$$

$$\text{Simplified Gamma:} \quad R = 1 - \frac{\gamma}{(\gamma + t)^p} \quad [2.8]$$

$$R = \frac{t}{g + t} \quad [2.9]$$

$$R = R_{\max} (1 - e^{-kt}) \quad [2.10]$$

$$\text{Fermentation model:} \quad R = \frac{R_{\max}}{(1 + k/t)} \quad [2.11]$$

R denotes cumulative recovery at time t and R_{\max} , k , γ , g and p are curve fitting parameters. As long as the chosen equation fits the data reasonably well with only two curve-fitting parameters, the choice of a particular model is often not critical (Klimpel, 1984b). This present work adopts expression [2.10] in which k is interpreted as the initial rate (min^{-1}) and R_{\max} the equilibrium recovery at long flotation times (the asymptote of the cumulative recovery-time curve at high t -values). According to Agar et al. (1980), this relationship can be applied to all the components of the flotation system including water. Through its use, a continuous circuit can be simulated from batch data, and all the more, the treatment time in the various stages can be optimised.

Despite the general awareness that flotation rate is an important variable, performance between different systems, for example reagent schemes have been generally assessed by only looking at differences in R_{\max} . Klimpel (1984a) has argued that this approach implies that flotation is an equilibrium process. Also, such an assumption suggests that differences in recovery measured in the laboratory will indicate recovery differences in the plant, regardless of the time-scale differences between the two. This is inconsistent with the findings of a testing program he conducted in order to determine some general guidelines for the use of chemicals in flotation plants. Klimpel (1984a) showed that the laboratory-scale time value (time equivalency value) to be used for comparing laboratory flotation results to the behaviour of the plant could be anywhere in the laboratory time scale. The time equivalency

value can be viewed as the time in the laboratory time-recovery profile that corresponds to the measured plant final recovery in the section under study. In some work conducted by this author, the appropriate laboratory time value was found to be considerably less than normally associated with equilibrium recovery. Figure 2.12 illustrates the fitting of typical lab data to the Klimpel model (equation [2.6] above) so as to characterise each profile by appropriate R and K parameters. If the plant being simulated corresponds to a laboratory time less than t_k , the settings associated with System 1 are preferred, while the converse is true if the laboratory equivalence value is greater than t_k (denoted as the R/K trade-off).

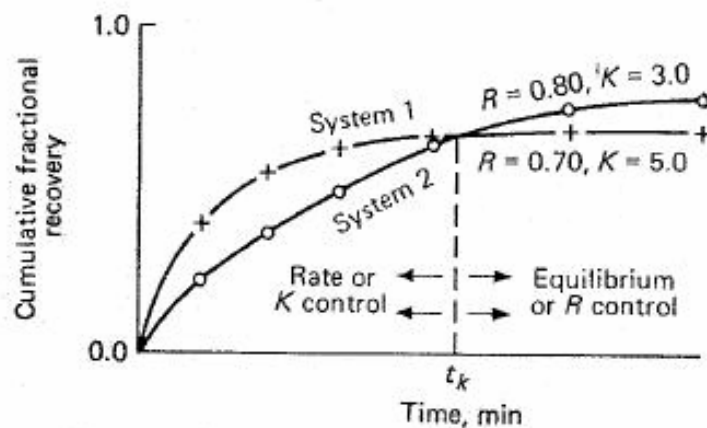


Figure 2.12 Typical curves obtained by fitting recovery-time data to a two parameter model. System 1 shows a high rate and low equilibrium recovery; System 2 shows the reverse (Klimpel, 1984b)

The recovery-time profiles in Figure 2.12 can be divided into two regions; the first where recovery is sensitive to the time of flotation is called rate control. The second is under equilibrium control and is where curve flattens and the recovery is not sensitive to time. Experience has shown that different reagent schemes used on the same ore give different curve shapes when their recovery-time data are fitted into a model such as shown in Figure 2.12. According to Klimpel (1984a), this is important because plant performance is often correlated with lab results for lapses of times considerably less than those corresponding to equilibrium recovery. The author concluded that the

most important difference between tests is often in the rate at which the valuable mineral can be removed from the cell. The K difference is crucial and can sometimes overwhelm the importance of the associated R difference.

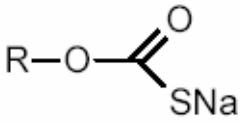
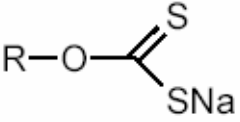
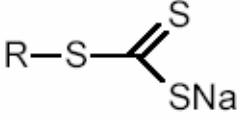
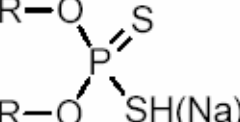
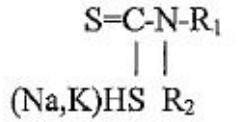
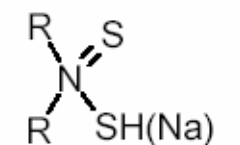
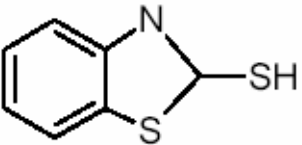
2.5. Collectors for Auriferous Pyrite Flotation

Thiols are the collectors most widely in used in the flotation of pyrite (O'connor and Dunne, 1994). Examples include dithiocarbonates, trithiocarbonates, dithiophosphates, dithiocarbamates, thionocarbamates and mercaptobenzothiazoles. Tables 2.5 and 2.6 show a summary of properties and applications of these reagents.

Table 2.5 *Application of Selected Thiol Collectors* (after Bradshaw, 1997)

Collector	Application and Properties
Dithiocarbonates (Xanthates)	- Used in a pH range of 8-12 - Undergo hydrolysis at low pH
Dithiophosphates	- More resistant to oxidation than xanthates and less stable than xanthates in moist conditions, and are usually stabilised with soda ash - Generally used at high pH, effective in the pH range 4-12 and used in mixtures with other collectors for high recoveries
Thionocarbamates	- Reasonably stable but hydrolyse in acidic conditions - Less sensitive to water chemistry than xanthates and dithiophosphates - Generally applied in the pH range 4-9
Thiocarbamates	- They have been known for a while but have not achieved much commercial success because they decompose readily in acidic conditions
Mercaptobenzothiazoles	Mostly used in combinations with DTP and/or xanthate for flotation of tarnished and oxidised ores and cyanidation tailings at low pH. These conditions promote removal of oxide and cyanide, which could interfere with interaction with reagents. The costly neutralisation step is not necessary because the collector operates efficiently at low pH.

Table 2.6 Selected Thiol Collector Structures (after du Plessis, 2003)

Collector	Structure
Monothiocarbonates	
Dithiocarbonates	
Trithiocarbonates	
Dithiophosphates	
Thionocarbamates	
Thiocarbamates	
Mercaptobenzothiazoles	

Dithiocarbonate and trithiocarbonate collectors, which are the focus of this present work, differ in the isomorphous substitution of sulphur for oxygen (Figure 2.13)

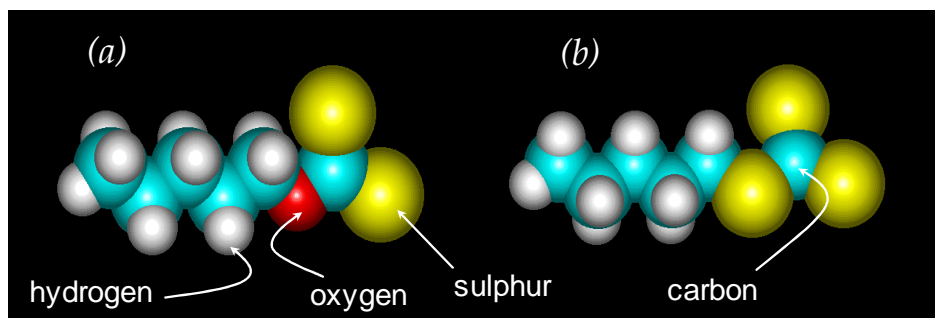


Figure 2.13 Thiol collectors (a) dithiocarbonates, (b) trithiocarbonates (Miller, 2003)

According to Fuerstaenau (1982a), increasing the length of the hydrocarbon group of collector molecules:

- Increases recovery power, frothing properties, mass recovery, water repulsion and the tendency to form micelles.
- Lowers selectivity and solubility

Micelles are stable reversible aggregates that are formed spontaneously when collector concentrations exceed a certain threshold known as the critical micelle concentration (CMC). In solution a three dimensional, regular array of the molecules results from intermolecular bonding. The shape taken by the assemblages depends primarily on surfactant architecture, the solvent, presence of added components (such as co-surfactants and salts) and temperature. Examples of assemblies are shown in Figure 2.14. In order to lower solution free energy, surfactants self-assemble by creating an interface separating the aqueous phase from the hydrophobic portions of the surfactant. The hydrophobic portions aggregate to form an oily interpenetrating assembly that is separated from the aqueous solvent by the hydrophilic head-group. The head-groups serve to define a boundary for double layer structure between the aqueous and oily pseudo-phases.

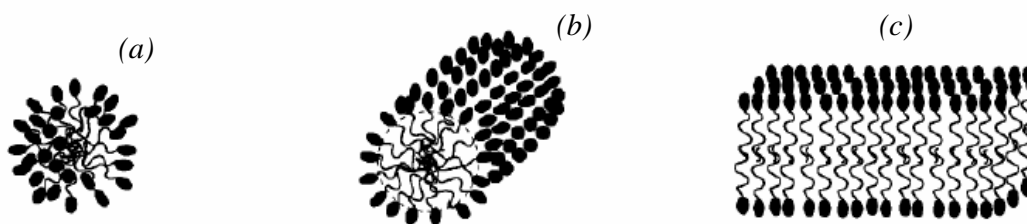


Figure 2.14 Illustration of different surfactant self-assembly structures (a) spherical micelle, (b) cylindrical micelle and (c) lamellar micelle (Boschkova, 2002).

When collector molecules are bonded to a surface, three dimensional arrays are not possible. Instead hydrophobic bonding dominates intermolecular attraction. In solution, dodecyl structures typically form micelles around 0.08M solutions (Davidtz, 2005). A typical monolayer surface of thiocarbonate collector is so dense that it can be compared with a solution at concentrations around 8M, three orders of magnitude higher than the CMC. For a nC_6 xanthate, interaction between neighbouring collector species begins at a surface density of coverage of about 0.7 (Slabbert 1985)

2.5.1 Xanthate (Dithiocarbonate) Collectors

The xanthates, first patented in 1925 are the most widely used flotation collectors and account for over 80% of world usage of thiol collectors (Crozier, 1992). Some factors contributing to this wide application are: they possess good water solubility and they are very stable in alkaline conditions. Xanthates are also inexpensive, easy to manufacture, transport, store and handle and they are very effective in the non-selective flotation of sulphides. This investigation uses SIBX, which is synthesised by reacting carbon bisulphide (CS_2), butyl alcohol (C_4H_9OH) and a strong alkali (NaOH):



The xanthate can also be produced by reacting ether with the alkali and carbon disulphide:



Xanthates undergo different reactions dependant on the environment they are exposed to (Figure 5.3). They may decompose via the hydrolysis reaction to xanthic acid and then to the original reactants, carbon bisulphide and alcohol (de Donato et al. (1989)).

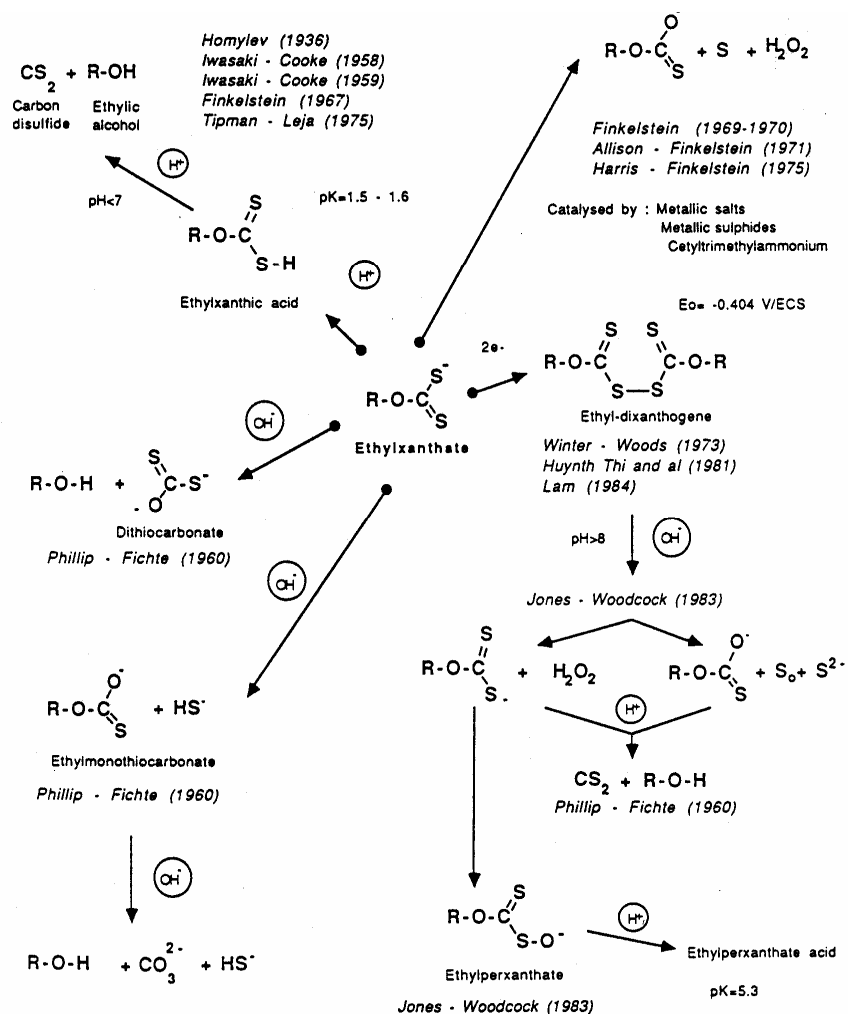


Figure 2.15 Hydrolysis and oxidation of ethyl xanthate in aqueous solution: the different reactive paths. R is the ethyl radical (de Donato et al., 1989)

The stability of xanthates in aqueous solutions depends on solution pH, the rate of decomposition decreasing with increasing pH. The flotation circuit at No 2 Gold Plant is run at a near neutral pH of 7.2 for which SIBX is expected to be stable.

Metallic sulphides and metal ions may catalyse the oxidation of xanthates to dixanthogen (Bradshaw, 1997). Xanthates are reducing agents that form ferrous and cuprous salts in the presence of iron and copper ions respectively. In cases where the iron is present in the ferric state, Fe^{3+} , the ferric xanthate that is initially formed is quickly reduced to ferrous xanthate (Sutherland and Wark, 1955). In practice, the effectiveness of xanthates increases with the molecular weight of their alcohol radical (Table 2.7).

Methyl xanthates are more effective on Cu, Hg and Ag minerals, and iron sulphides. Ethyl and the C_3 to C_5 xanthates are effective in normal concentrations without the need for activators for all heavy metal sulphides except sphalerite and pyrrhotite. The failure to collect these two is due to the ferrous and zinc compounds formed by C_1 to C_5 xanthates being soluble at economic reagent quantities.

Table 2.7 Response of sulphide minerals to collectors of the xanthate type (Marsden and House, 1992)

Collector \ Mineral	Methyl Xanthate	Sodium Aerofloat	Ethyl Xanthate	Butyl Xanthate	Amyl Xanthate	Hexadecyl Xanthate	Potassium di-amyl dithio-carbamate
Sphalerite Pyrrhotite	Response To Collectors Only In The Presence Of Activators						
Pyrite Galena Chalcopyrite							
Bornite Covellite Chalcocite	Response To Collectors Without Activation						

2.5.2 Xanthate – Pyrite Interactions

The mechanisms by which xanthates float pyrite have been studied extensively over the years and Wang (1994) lists some of this work. The traditional theory considers xanthate adsorption as an electrochemical process that involves the formation of dixanthogen (Chander, 1999). This conclusion has been drawn from spectroscopic (Fuerstenau et al., 1968), electrochemical (Woods, 1976; Usul and Tolun, 1974; Majima and Takeda, 1968) and flotation data (Fuerstenau et al., 1968). The sole presence of dixanthogen on the pyrite surface after contact with xanthate has been demonstrated clearly using infrared spectroscopy (Figure 2.16).

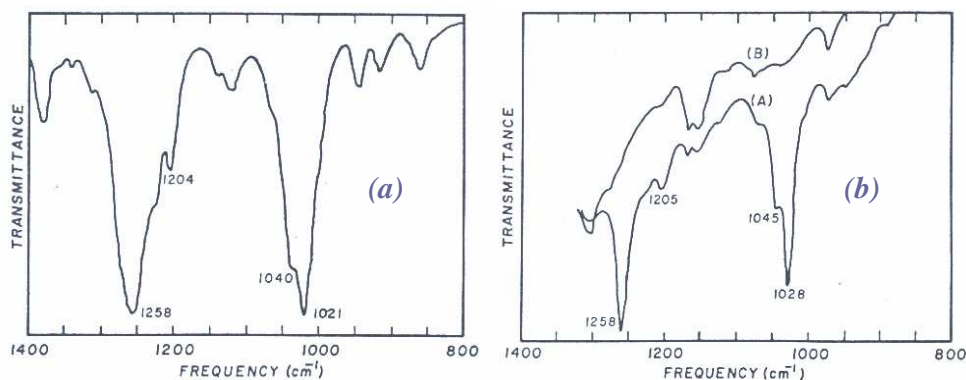


Figure 2.16 Infrared spectrum of (I) diamyl dixanthogen, (II) pyrite conditioned at pH 3.5 in the absence (Curve B) and presence (curve A) of potassium amyl xanthate (after Fuerstenau et al., 1968)

The principal absorption bands of diamyl dixanthogen occur at 1,021 and 1,258 cm^{-1} (Figure 2.16 (a)). After contact with amyl xanthate, the principal absorption bands of pyrite occur at 1,028 and 1,258 cm^{-1} (Figure 2.16 (b)), which correspond closely with those of dixanthogen.

The formation of dixanthogen is also supported by measurements of pyrite rest potentials in various xanthate solutions (Alison and Finkelstein, 1971), which are close to xanthate/dixanthogen redox couples (Crozier, 1991). Electrochemical interactions between sulphides and xanthate collectors that

result in dixanthogen formation were first suggested by Salamy and Nixon (1952). They postulated that oxidation of collector ions occurs at anodic sites according to:



This reaction being supported by a cathodic reduction of adsorbed oxygen:



As emphasised by de Wet et al. (1997), initial attachment of the xanthate onto pyrite before the oxidation to dixanthogen is important. These authors cited the work by Ackerman et al. (1987) in which pyrite responded poorly to flotation with dissolved dixanthogen. They also referred to the findings by Leppinen (1990) who used in-situ spectroscopic techniques to show that a monolayer of iron xanthate initially adsorbed on pyrite, after which dixanthogen formed just above it.

Based on Fourier Transform Infra Red (FTIR) spectroscopic studies, Wang (1994) has shown that pyrite-xanthate interactions result in the formation of ferric xanthate as well. Figure 2.17 shows the differential spectra of ethyl xanthate treated pyrite. Two intense absorption peaks can be observed at 1252 and 1030 cm^{-1} . Comparison of spectra in Figure 2.17 with that of dixanthogen and ferric xanthate in Figure 2.18 shows the presence of diethyl dixanthogen. Other absorption bands at 1250 and 1005 cm^{-1} are close to those of ferric ethyl xanthate (Figure 2.18 (b)), suggesting it is one of the surface products formed when xanthate ions are adsorbed.

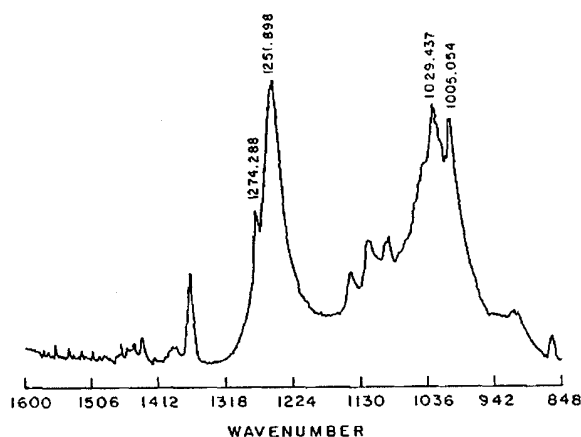


Figure 2.17 Differential IR spectrum of pyrite after reacting with 1.0×10^{-3} mol/l sodium ethyl xanthate solution at pH 6 (after Wang, 1994).

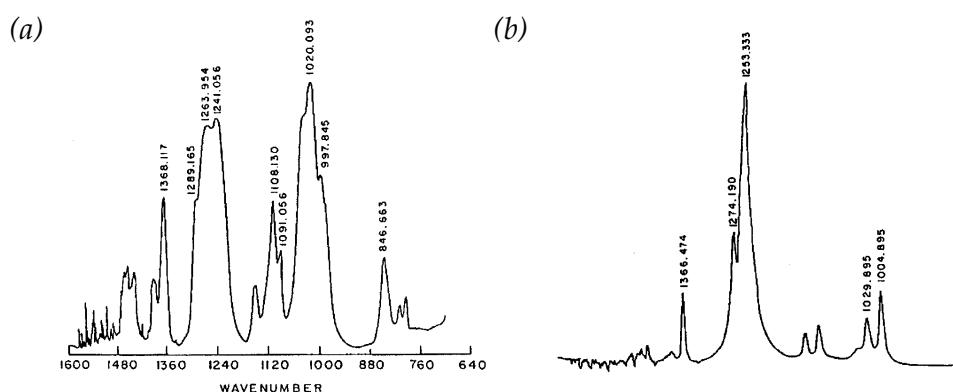


Figure 2.18 FTIR of (a) diethyl dixanthogen and (b) ferric ethyl xanthate, both in KBr (Wang, 1994)

2.5.3 Trithiocarbonate Collectors

TTCs can be of either ionic (Figure 2.19 (a)) or ester (Figure 2.19 (b)) type. The former is chemically known as alkyl trithiocarbonate and both the straight and branched chains are recognized. TTCs are synthesized by dissolving an alkali hydroxide in the appropriate alkyl mercaptan, followed by the addition of carbon disulphide to the resulting metal mercaptide:





Generally, freshly prepared sodium and potassium salts are bright yellow in colour and possess a distinct odour. The differences between the straight and branched chains are not yet fully understood, and the latter seem to be superior, (du Plessis et al., 2000).

Studies have shown that the ester-type TTCs are very effective in the bulk flotation of sulphide minerals (Coetzer and Davidtz, 1989). Their higher cost however seems to discourage their application so that ionic TTCs are preferred.

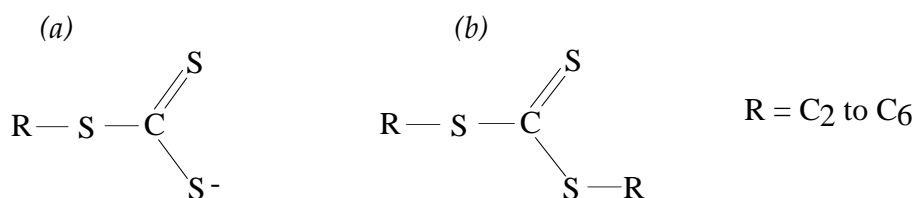


Figure 2.19 Chemical structure of (a) ionic TTCs and (b) ester type ionic TTCs

2.5.4 TTC – Pyrite Interactions

The flotation of pyrite by xanthate collectors is known to occur through the formation of metal xanthates (Wang, 1994) and then dimers (Chander 1999). Oxidation of TTC molecules to their dimers (Figure 2.20), supported by the cathodic reduction of oxygen (equation 2.15), may occur on mineral surfaces, selectively rendering them hydrophobic. Supporting evidence for this assertion can be obtained from FTIR spectroscopy (du Plessis, 2003). Figure 2.21 compares the FTIR transmission spectrum of a TTC dimer with an external reflection FTIR spectrum of a pyrite surface treated with TTC under oxidizing conditions. It is clear that there is good agreement between the two, indicating bulk dimer formation at the pyrite surface.

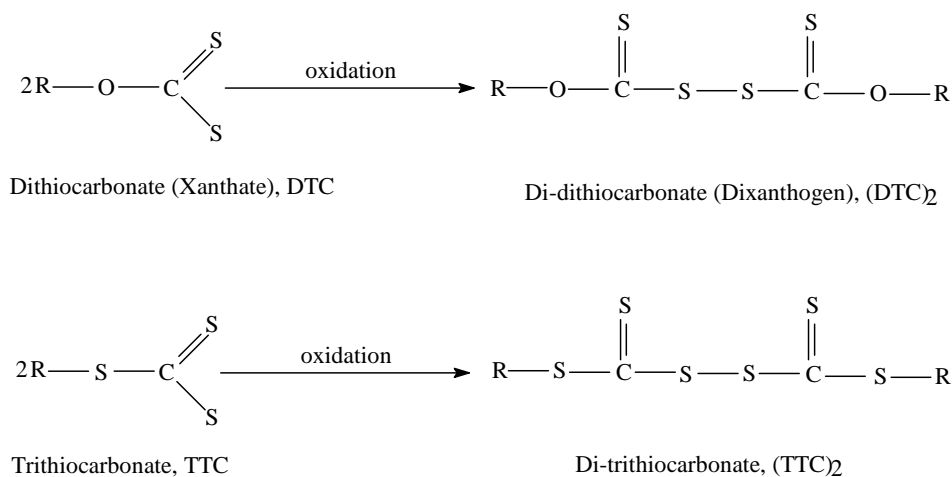


Figure 2.20 Oxidation of Trithiocarbonates to their corresponding dimers (du Plessis et al., 2000)

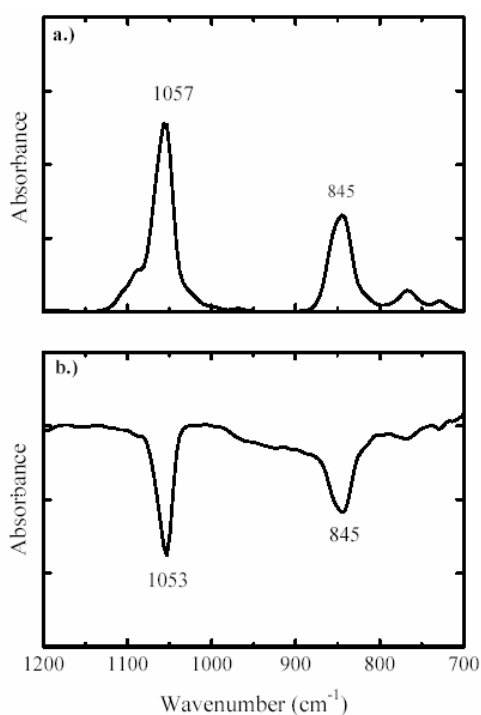


Figure 2.21 (a) FTIR transmission spectrum of the *n*-amyl trithiocarbonate dimer compared to (b) the FTIR external reflection spectrum of pyrite treated with 1 × 10⁻³ M potassium *n*-amyl trithiocarbonate, at 0.1 V for 15 minutes at pH 4.7 in air (45°, *p* polarized) (du Plessis, 2003).

The work conducted by du Plessis *et al.* (2000) has further shown that TTC collectors oxidise more readily^x the higher the number of sulphur atoms in their functional group (Figure 2.22)

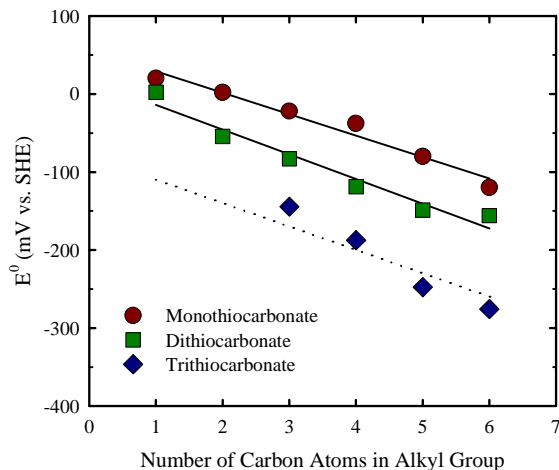


Figure 2.22 Standard reduction potentials for thiocarbonate collectors as a function of alkyl chain length (after du Plessis *et al.*, 2000)

TTCs have been reported to be stronger collectors than DTCs and can be used at lower dosages for near neutral pH slurries (Klimpel, 1999; Coetzer and Davidtz, 1989). Research by Sutherland and Wark (1955) has shown that an increase in the number of sulphur atoms in the functional group of thiol collectors improves their tendency to adsorb on sulphide mineral and metal surfaces. Work conducted by Slabbert (1985) on the flotation of PGMs from a Merensky ore (South Africa) using iC_3 TTC collector showed an increase in recovery relative to a mixture of xanthate and dithiophosphate. A monoalkyl trithiocarbonate (Orfom 800) developed by Philips Petroleum Company has been used as a collector in the flotation of copper ores in the USA and in Spain (Avotins *et al.*, 1994). It is against this background that this work seeks to test the flotation with TTC collectors, of pyrite and gold from leach residues being treated by AngloGold Ashanti's North No. 2 Gold Plant.

^x A lower value of E_h^o indicates that the collector oxidises more readily

2.5.5 Synergism in SIBX/TTC Mixtures

Although benefits have been reported for a wide range of collector mixtures, the mechanisms of enhancement have not been clearly established (Bradshaw, 1997). Some authors have attributed better performance to the summation of individual contributions of the respective collectors (Mitrofanov et al., 1985). Others have however ascribed it to synergism, the working together of two collectors to yield flotation performances greater than the sum of the individual reagents. A typical illustration is the work conducted by du Plessis et al. (2000) in which a mixture of 25% C₁₂ TTC and 75% SIBX gave better sulphide flotation response than SIBX (Figure 2.23).

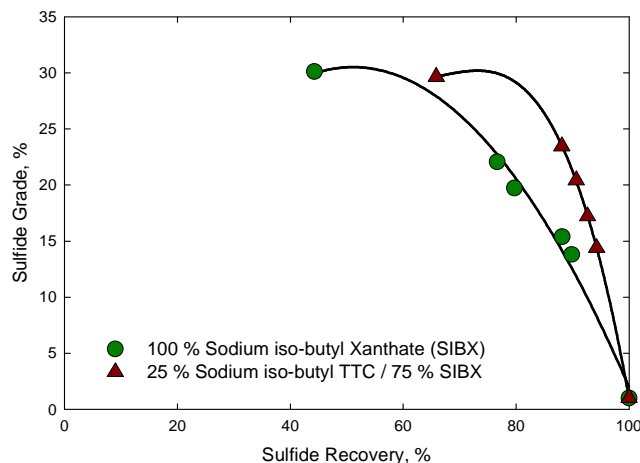


Figure 2.23 Grade–recovery curves evaluating iso-butyl dithiocarbonate and a 25% iso-butyl Trithiocarbonate / 75% iso-butyl dithiocarbonate mixture for auriferous pyrite recovery with air at pH 8 (du Plessis et al., 2000)

2.5.3.1 Mechanisms of Synergism

Early work by Plaskin et al. (1954) into the effect of using blends of ethyl xanthate and amyl xanthate in the flotation of arsenopyrite and galena recorded recoveries that were higher than simple summations of individual effects by pure collectors. The authors attributed this to better adsorption on mineral surfaces that were viewed as inhomogeneous. The improved flotation

responses were also accompanied by higher recovery kinetics for all collector mixtures tested. In single-point flotation tests of a mixed copper ore with various mixtures of dithiophosphates, monothiophosphates and xanthates, Mitrofanov et al. (1985) reported improved collection of fines due to the combination of the frothing properties of dithiophosphates and the “dry” froth produced by xanthates. Critchley and Riaz (1991) reported enhanced microflotation of heazlewoodite with a 1:2 mixture of potassium ethyl xanthate and diethyl dithiocarbamate and ascribed it to enhanced overall extent of collector adsorption. Valdiviezo and Oliveira (1993) used surface tension measurements correlated to contact angle measurements to show that synergism existed between a 3:1 molar ratio of ethyl xanthate and sodium oleate. They attributed this behaviour to a favourable arrangement of the species on mineral surfaces.

A literature survey conducted by Bradshaw (1997) summarised that the synergistic enhancement of flotation observed for many collector blends has been largely attributed to improved adsorption characteristics of the mixed collectors on mineral surfaces as compared to pure collectors. The author highlighted the work conducted by Mellgren (1966) who proposed that when one of the collectors adsorbs by chemisorption, it provides sites on the mineral surface for the subsequent adsorption of the second collector, which is comprised of more hydrophobic neutral molecules, thereby increasing the overall hydrophobic properties of the mineral.

This means that for the SIBX – TTC mixtures being tested in this present work, one of the two, possibly TTC could initially irreversibly adsorb and the dithiolate of SIBX could increase the density of collector packing by physisorption and thereby increase the hydrophobic state of the sulphide surface (Davidtz, 2002).

2.6. Activators for Auriferous Pyrite Flotation

Activators are generally soluble salts that ionise in solution; the ions then react with the mineral surface and promote collector adsorption. Work done by Miller (2003) indicates that lead (II) in lead nitrate can be used to activate auriferous pyrite in pulps containing traces of cyanide. These conclusions are based on contact angle measurements (Figure 2.24) and maybe due to the fact that Pb^{2+} ions do not complex with cyanide. The implication is that Pb ions can activate pyrite promoting xanthate adsorption.

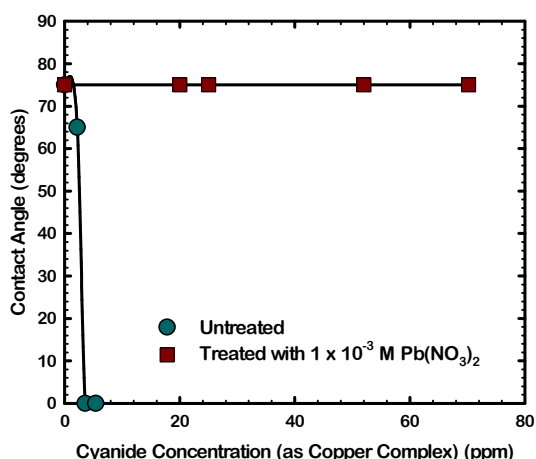


Figure 2.24 Electrochemically controlled contact angle measurements as a function of lead concentration for pyrite in $1 \times 10^{-3} M$ PAX solution, pH 4.7, at a potential of $-300 mV$ vs. SCE (Miller, 2003)

The investigation by Miller (2003) was conducted at pH 4.7 and a potential $-0.300 mV$ (SCE), which translates to $-0.032 V$ (SHE). This coincides with the domain in which Pb^{2+} is thermodynamically stable (Figure 2.25 (a)). The speciation diagram plotted for the lead concentration that Miller (2003) used shows that approximately 90% of lead is in the Pb^{2+} form at pH 4.7.

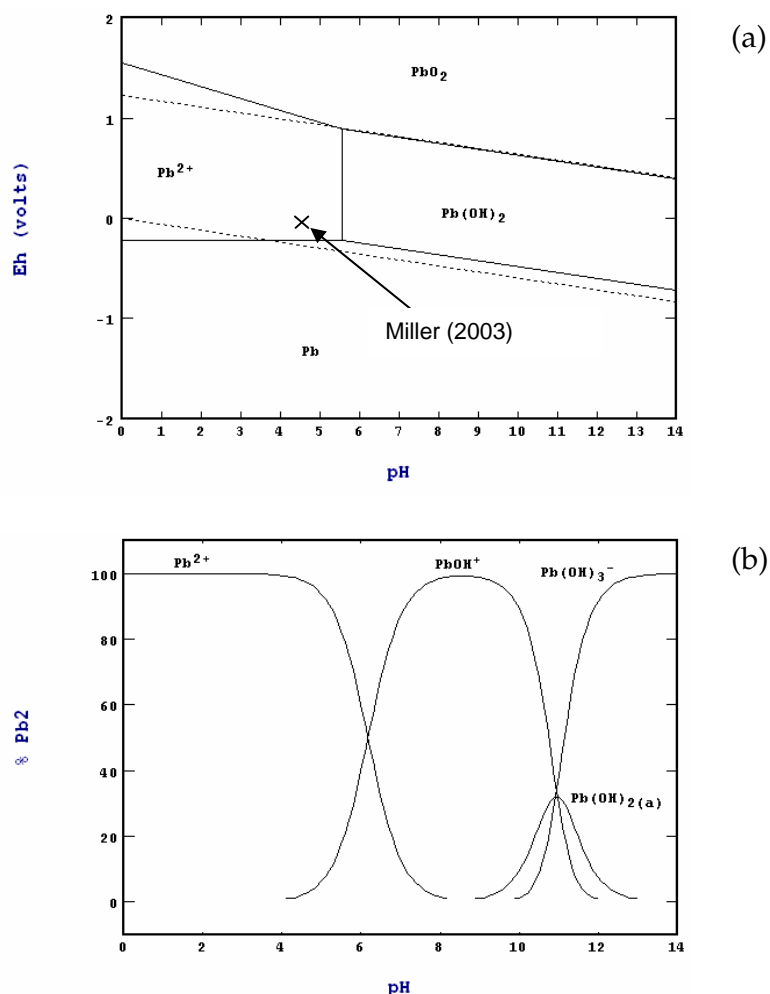


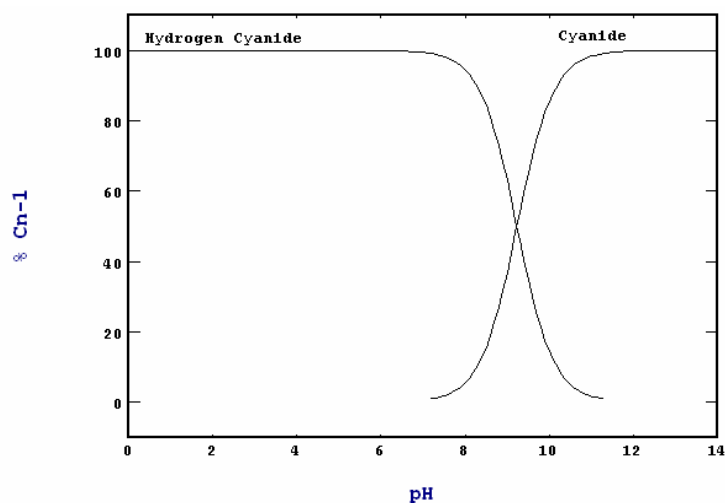
Figure 2.25 (a) A Pourbaix diagram for the Pb-H₂O system at $1 \times 10^{-3} \text{M}$ [Pb²⁺] showing E_h -pH conditions used by Miller (2003), (b) Lead (II) speciation at $1 \times 10^{-3} \text{M}$ [Pb²⁺]. Diagrams drawn with STABCAL software using NBS database

If the Pb²⁺ state is a pre-requisite for lead nitrate to be an effective activator, then flotation must be conducted at relatively low pH (Figure 2.25 (b)). Running a flotation circuit in acidic conditions is however likely to be detrimental to xanthate collectors if residence times are long. The work conducted by Viljoen (1998) shows that in air, the xanthate has a half life of 63.2 hours at pH 6 (Table 2.8). Cyanide too may hydrolyse to give HCN (equation 2.18), a poisonous gas at these low pH values (Figure 2.26).



Table 2.8 Half-life times for SIBX and iC_3 -TTC for different gaseous environments and pH (Viljoen, 1998)

Collector	Half life			
	pH 6		pH 9	
	N ₂	Air	N ₂	Air
SIBX	81.5 hours	63.2 hrs	1172 hours	1193 hours
iC_3 -TTC	25 minutes	36 minutes	40 minutes	63 minutes

**Figure 2.26** Proportion of cyanide species present as a function of pH at $2 \times 10^{-3} [CN^-]$. Diagram drawn using STABCAL Software, NBS Database

2.6.1 Adsorption of Lead (II) Ions on Pyrite

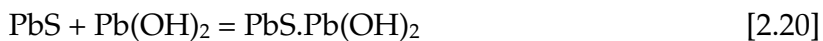
Sui et al. (1997) used cyclic voltammetry at a sweep rate of 20mV/s from -800mV to 300mV (SCE) to compare the behaviour of lead-treated pyrite and clean pyrite at pH 10.5. Both samples yielded similar voltammograms, which was attributed to lack of significant electron transfer between adsorbed lead ions and pyrite within the potentials tested. Based on this finding, the authors concluded that lead-uptake was through physisorption. At low pH, Allison (1982), Wang et al. (1989) and Leppinen et al. (1995) also showed that activation of pyrite did not involve cationic exchange between lead in solution

and the sulphide lattice. Inspection of the lead speciation diagram in Figure 2.35 shows that Pb^{2+} dominates at low pH while at pH 10.5, approximately 60% is in the form of $PbOH^+$, 28% as aqueous $Pb(OH)_2$ and 12% as $Pb(OH)_3^-$. Therefore regardless of pH and the lead species present, uptake of lead by pyrite only involves physisorption. It is important to note that the $Pb(OH)_3^-$ species depresses galena (Fuerstenau, 1982b) so that it should affect pyrite similarly. However, since it only forms 12% of the total lead, its effect could be small. Therefore, the interaction of lead-treated pyrite with xanthate recorded by Sui et al. (1997) could be a result of $PbOH^+$ and aqueous $Pb(OH)_2$ species only.

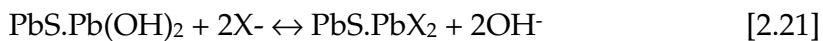
Sui et al. (1997) also showed that at pH 10.5, open circuit potentials (rest potential) of clean pyrite and lead-treated pyrite were similar. They suggested the electrochemical properties of pyrite were not significantly altered by the presence of Pb ions. Compared to clean pyrite, a pyrite electrode treated with 20ppm $PbCl_2$ showed two peaks in the presence of $10^{-3}M$ xanthate at pH 10.5, an anodic peak at 100mV that they attributed to formation of $Pb(OH)X$ and dixanthogen and a cathodic peak at -750mV due to dixanthogen reduction. The magnitude of the current at 100mV did not change for all lead concentrations tested (between 1 and 100ppm), leading to the conclusion that the electrode was already saturated at 1ppm lead. Pyrite contacted with a supernatant from a galena particle bed gave a similar voltammogram with that treated with $PbCl_2$. This means that Pb ions play the same role in promoting pyrite interaction with xanthate irrespective of their source.

Infrared spectra obtained from lead-treated pyrite exposed to xanthate showed a more intense dixanthogen peak compared to clean pyrite, which shows lead activated pyrite and was consistent with voltammetric results in which dixanthogen formation was inferred. The interaction between lead-treated pyrite and xanthate could be similar to the mechanism proposed by O'Dea and co-workers (2001) in their study of xanthate adsorption on galena

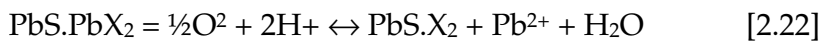
at high pH. Lead (II), which is predominantly in hydroxide form due to hydrolysis is attached to the surface:



An exchange reaction between xanthate and hydroxide may then take place:



Oxidation of xanthate to dixanthogen accompanied by oxygen reduction may follow:



It is likely that $\text{Pb}(\text{OH})_2$, which forms 60% of lead (II) species at pH 10.5 adsorbs onto pyrite and undergoes similar reactions as shown above, with pyrite taking the role played by galena.

2.6.2 Copper Sulphate

Under neutral pH conditions, pyrophyllite or the so-called khaki shales in most ores from the Witwatersrand basin do not float readily. Copper sulphate additions ensure that pyrite flotation is not depressed. Some flotation circuits recovering pyrite together with uranium bearing minerals operate at low pH levels (O'Connor et al., 1988). Under these conditions, the addition of copper sulphate enhances the rate of pyrite flotation, concentrate grade and reduces conditioning time. Typical addition rates vary between 30g/t and 100g/t, (O'Connor and Dunne, 1991), with even higher rates being applied in the treatment of refractory ores. Conditioning times are generally less than 1 minute.

A number of theories have been proposed to explain the mechanism of pyrite activation. O'Connor and co-workers (1988) have drawn attention to some of this work. Livshits and Dudenkov (1965) showed that the insoluble hydrophobic precipitates formed by xanthates in the presence of Cu^{2+} ions destabilise the froth phase. It has often been suggested that the addition of copper sulphate activates pyrite in streams containing traces of cyanide by forming copper-cyanide complexes. Westwood et al. (1970) and Lloyd (1981) however disputed this; with Westwood and co-workers arguing that although copper complexes with cyanide, the addition of copper sulphate alone is insufficient, low pH is also required. Work done by Levin and Veitch (1970) reported poor results from laboratory batch flotation tests in which CuSO_4 was added as compared to ones in which no addition was made, thus suggesting that the presence of copper ions jeopardised the process. In flotation plants however, the exclusion of copper sulphate has been shown to give overall poorer performance (Broekman et al., 1987).

O'Connor et al. (1988) carried out adsorption studies of copper sulphate on onto gravity concentrated pyrite containing quartz and khaki shale gangue.

Their results are shown in Figure 2.27. Tests 1, 2 and 3 were carried out under identical conditions, as were tests 4, 5 and 6. Figure 2.28 shows the grade-recovery data for the same set of tests. Despite the poor reproducibility in tests 4-6, it is clear that the addition of copper sulphate enhanced both pyrite grades and final recoveries. In addition, Figure 2.29 shows that gangue recovery increased due to the dosing of copper sulphate.

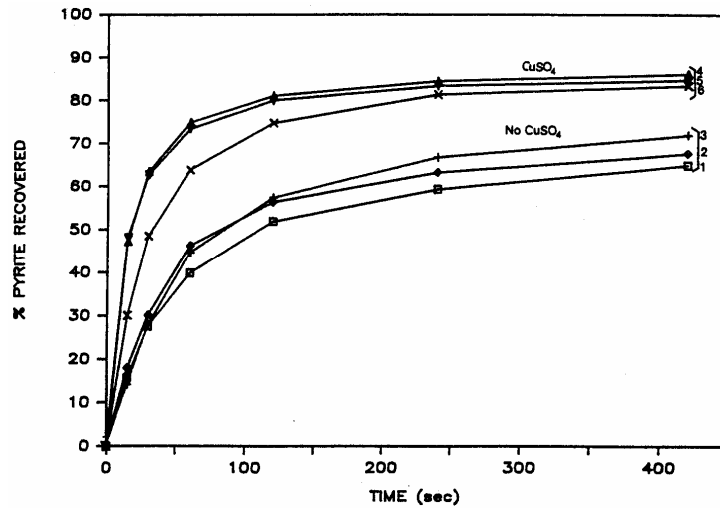


Figure 2.27 Effect of copper sulphate on recovery of pyrite (O'Connor et al., 1988)

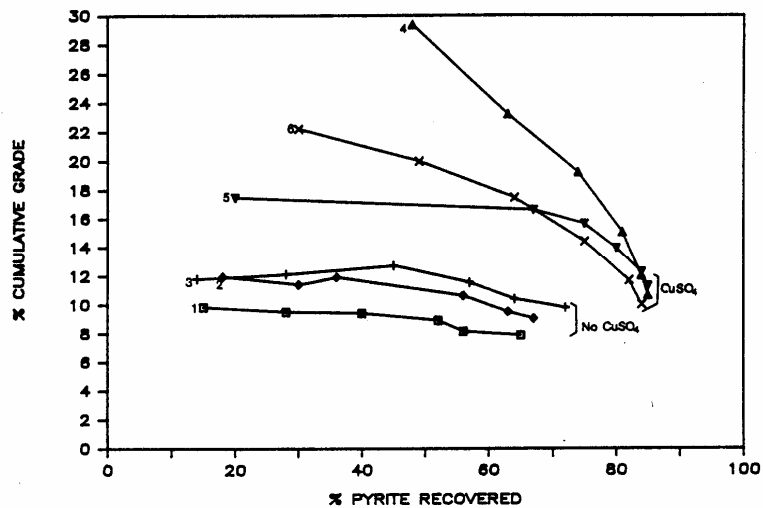


Figure 2.28 Effect of copper sulphate on pyrite flotation (O'Connor et al., 1988)

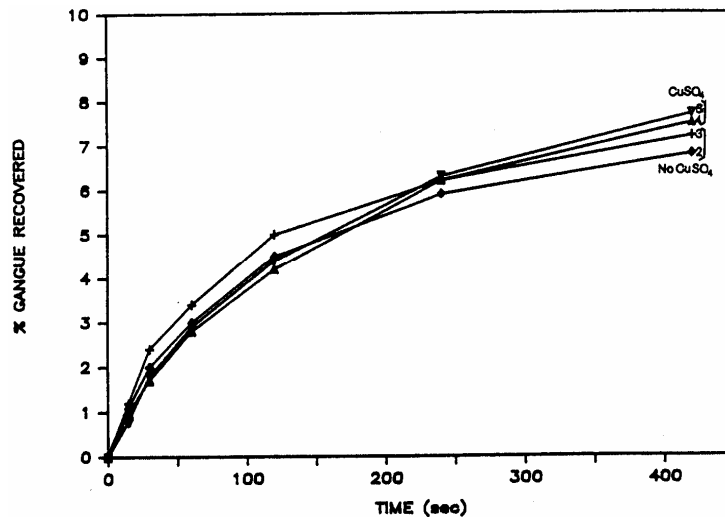


Figure 2.29 Effect of copper sulphate on gangue recovery (O'Connor et al., 1988)

2.6.3 Adsorption of Copper (II) ions on Pyrite

Several theories regarding the mechanism by which copper (II) activates pyrite have been put forward and a literature survey conducted by Chen (1999) lists some of this work. Allison (1982), Wang et al. (1989) and Leppinen et al. (1995) studied the activation of pyrite by heavy metal ions and showed that the adsorption of Cu^{2+} on pyrite did not involve exchange with the lattice cation. They concluded that it was the hydroxides that adsorbed on pyrite during the initial stage of activation. Wang et al. (1989) and Voigt et al. (1994) also agreed that the activation products were CuS_2 or $(\text{Cu}, \text{Fe})\text{S}$, together with surface cupric hydroxide which interacted with ferric hydroxides resulting from the oxidation of the pyrite surface. The adsorbed cupric hydroxide was found to dissolve readily in water. Voigt and his co-workers studied the relationship between the adsorbed cupric hydroxides and cuprous sulphides. They found that the adsorption in the cuprous form was independent of pH, whereas the adsorption of the cupric form rose sharply with the pH and reached a peak at about 9. They also observed that the adsorption of the cupric hydroxide had an induced stage: copper (II) was detected at the surface only after it had been

exposed to the activating solution for about 15 minutes. It took about 2 minutes for copper (II) to reach its maximum density at the surface at pH 5; at pH 10 it took far longer. At pH 10, copper (I) seemed to form in two distinct stages, the second stage started only after the adsorption of the hydroxide had commenced. This study showed that the activation of sulphide minerals under alkaline conditions involves complex interactions between the sulphide products, which are thought to be responsible for activation of the reaction with the collectors, and the hydroxides which are formed through oxidation of the mineral surface and hydrolysis of the activating ion. Voigt et al. (1994) also found the amount of copper adsorbed on pyrite, measured by the atomic surface ratio Cu/S, to be limited. The copper (I) did not exceed a monolayer on pyrite and did not penetrate below the surface.

Bushell et al. (1961), on the other hand, proposed that pyrite is activated with copper (II) by a reaction that essentially involves oxidation of pyrite with the formation of elemental sulphur:



Zhang et al. (1997) observed a significant increase in the zeta potential of pyrite after it was contacted with cupric ions at pHs above 6. Basing their argument on stability diagrams, they attributed this to uptake of $\text{Cu}(\text{OH})^+$. Upon addition of xanthate, the zeta potential decreased significantly. This was thought to be due to either adsorption of a negatively charged species and/or partial removal of adsorbed cupric ions from the pyrite surface. However, they observed increased pyrite recoveries, which suggested that the former was more likely. The presence of a positive charge from adsorbed cupric ions attracts negatively charged xanthate ions. The authors also used infrared spectroscopy to identify the surface species resulting from interactions pyrite treated with cupric ions and xanthate. Compared to

untreated pyrite, treated pyrite showed increased intensity of dixanthogen bands and additional bands which were attributed to cupric xanthate.

2.6.4 Cyanide and Activation of Pyrite with Copper and Lead Ions

The feed to No 2 Gold Plant consists of a mixture of tailings from cyanidation plants treating run-of-mine ore and reclaimed dump material. Leaching is carried out in alkaline conditions, typically above pH 10. The cyanidation reaction requires oxygen and common plant practice involves blowing air into leach pulps. This increases the amount of dissolved oxygen so that any sulphides present are prone to surface oxidation. Consequently, feed to the flotation circuit always contains oxidised pyrite as well cyanide carried over from leaching. The superficial oxide inhibits interaction with flotation reagents (Benzaazoua and Kongolo, 2002) and cyanide depresses pyrite (de Wet et al., 1997; O'Connor et al., 1988; Janetski et al., 1977, Elgillani and Fuerstenau, 1968).

Examination of the Pourbaix diagram of the Fe-S-CN-H₂O system (Figure 2.30) shows that ferricyanide ($\text{Fe}(\text{CN})_6^{3-}$) and ferrocyanide ($\text{Fe}(\text{CN})_6^{4-}$) are the stable species formed at the flotation pH of 7.2 used at No 2 Gold Plant. According to Seke (2005), most flotation processes are run at pulp potentials that thermodynamically favour the formation of ferrocyanide so that when the flotation feed enters the plant, it is likely to be adsorbed on pyrite. Elgillani and Fuerstenau (1968) have attributed the depression of pyrite by cyanide to the formation of this iron cyanide followed by the precipitation of ferric ferrocyanide ($\text{Fe}_4[\text{Fe}(\text{CN})_6]_3$) on the sulphide surface.

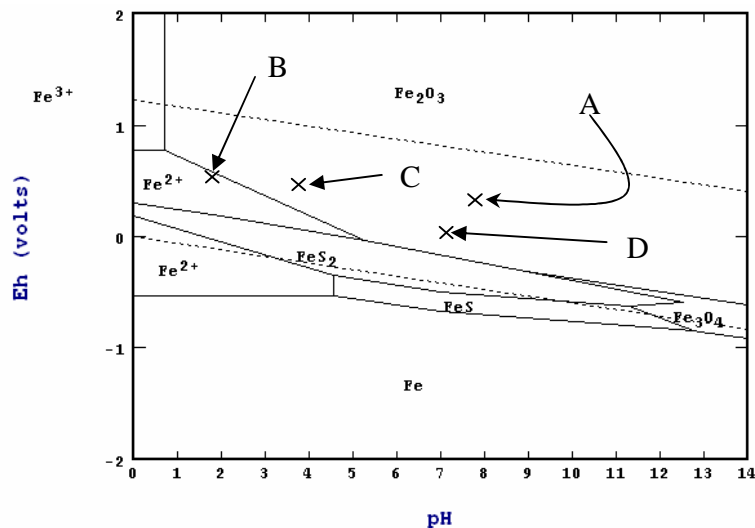


Figure 2.30 A Pourbaix diagram for the Fe-S-CN-H₂O system drawn using STABCAL software for $10^{-4}\text{M} [\text{S}]$, $10^{-4}\text{M} [\text{Fe}]$ and $2 \times 10^{-3}\text{M} [\text{CN}^-]$, NBS Database

The speciation diagram of copper (II) in Figure 2.31 predicts that at the plant flotation pH of 7.2, approximately 80% of the copper is available in the form of Cu^{2+} . Since this species dominates to a large extent, Cu^{2+} is likely to determine the behaviour of copper (II) in the flotation process.

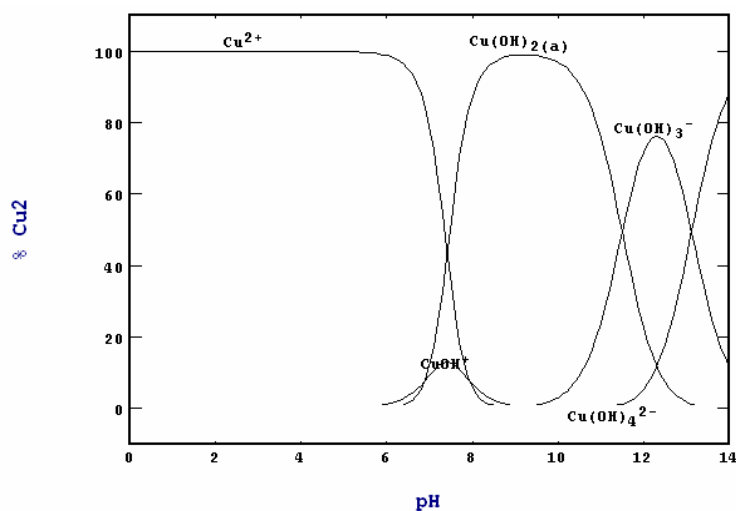


Figure 2.31 Copper (II) speciation at different pH values. Diagram drawn using STABCAL Software for $2 \times 10^{-4}\text{M} [\text{Cu}^{2+}]$, NBS Database

Since ferrocyanide is formed at E_h-pH conditions in which pyrite flotation takes place, any interaction between Cu²⁺ and ferrocyanide will affect the capacity of copper sulphate to activate pyrite. The work conducted by Bellomo (1970) in which copper (II) was titrated with ferrocyanide shows that the two interact to yield a reddish brown precipitate of copper ferrocyanide (Cu₂Fe(CN)₆) according to:

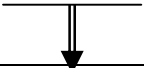
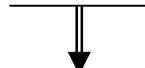


Considering the negative free energy change, it is reasonable to assume that copper ferrocyanide is formed spontaneously when copper sulphate is dosed to the flotation feed. The precipitate has a solubility of 2×10^{-6} mol/L and the plant doses 70g/t copper sulphate (equivalent to 2×10^{-4} M [Cu²⁺]). Since this is greater than the solubility, some of the salt formed should precipitate. It therefore appears that copper sulphate dosed in the presence of cyanide is likely to be consumed in the formation of copper ferrocyanide salt so that none is available to adsorb on pyrite and activate it. Consequently, xanthate cannot adsorb and pyrite will still be depressed. Perhaps this is the reason why Westwood and co-workers (1970) have emphasised that in flotation feed containing traces of cyanide, treatment with copper sulphate alone is not sufficient to render pyrite floatable. Low pH treatment is essential as well. The low pH probably destroys cyanide (Table 2.2), completely eliminating the participation of ferrocyanide so that Cu²⁺ can adsorb and activate pyrite without any interference from complex ion formation.

At No. 2 Gold Plant, cyanide is destroyed by treating flotation feed with calcine water, a low pH SO₂-containing solution (Table 2.2) prior to flotation. This reduces cyanide concentrations from about 125ppm to less than 4ppm (Brooks, 2005). The treatment is based on the INCO SO₂/AIR process

(Davidtz, 2002). Robins (1996) has outlined its basic chemistry and it consists of primary and secondary reactions and is shown in Table 6.2.

Table 2.9 Basic chemistry of the INCO SO₂/AIR process (Robbins, 1996)

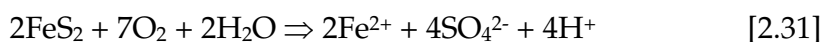
<i>Oxidation</i>	
$\text{CN}^-_{\text{free}} + \text{SO}_2 + \text{O}_2 + \text{H}_2\text{O} \rightarrow \text{OCN}^- + \text{H}_2\text{SO}_4$	[2.24]
$\text{Me}(\text{CN})^{2-}_4 + 4\text{SO}_2 + 4\text{O}_2 + 4\text{H}_2\text{O} \rightarrow 4\text{OCN}^- + 4\text{H}_2\text{SO}_4 + \text{Me}^{2+}$	[2.25]
$\text{Me}^{2+} = \text{Zn}^{2+}, \text{Cu}^{2+}, \text{Ni}^{2+}, \text{Cd}^{2+}, \text{etc}$	[2.26]
<i>Neutralisation</i>	
$\text{H}_2\text{SO}_4 + \text{Ca}(\text{OH})_2 \rightarrow \text{CaSO}_4 \cdot 2\text{H}_2\text{O}$	[2.27]
<i>Precipitation</i>	
$\text{Me}^{2+} + \text{Ca}(\text{OH})_2 \leftrightarrow \text{Me}(\text{OH})_2 + \text{Ca}^{2+}$	[2.28]
	
$2\text{Me}^{2+} + \text{Fe}(\text{CN})^{2-}_6 \leftrightarrow \text{Me}_2\text{Fe}(\text{CN})_6$	[2.29]
	
Reactions catalysed by copper in solution	
$\frac{\text{SO}_2}{\text{CN}_{\text{WAD}}} = 2.46\text{g/g}$	[2.30]

Weak dissociable cyanide (CN_{WAD}), which includes free cyanide and weakly complexed metal cyanides is oxidised to produce cyanate (OCN^-) and sulphuric acid. This reaction requires a small amount of copper in solution to serve as catalyst. Acid produced in the oxidation reactions is neutralised with lime.

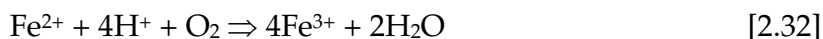
Due to the characteristic low pH of calcine water (typically 1.8), dosing it to plant feed also aids pyrite flotation by removing superficial oxide. This is formed during cyanidation and more significantly, during the period prior to excavation of the fraction of feed coming from old slimes dams (Dumisa, 2002). Examination of the Pourbaix diagram for the Fe-S-CN-H₂O system (Figure 2.30) shows that if E_h -pH conditions are adjusted to suit the domains in which ferric and ferrous ions are thermodynamically stable, then iron (III)

oxide (Fe_2O_3) should dissolve, exposing fresh sulphide that can interact freely with flotation reagents.

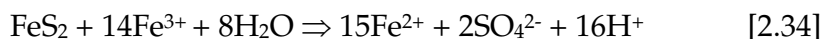
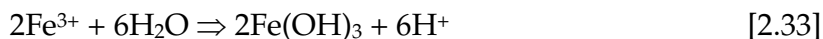
Apart from the beneficial destruction of cyanide and 'polishing' of sulphides, addition of calcine water introduces ferric and ferrous ions. In the presence of water, pyrite also undergoes oxidation. Jiang et al. (1998) have outlined the chemistry of the process, and the initial stage involves the production of ferrous ions:



The ferrous ions are oxidised to ferric ions due to the presence of dissolved oxygen and acid:



Ferric iron may undergo hydrolysis to form ferric hydroxide (equation 6.16), or it may oxidise pyrite to release more ferrous ions into solution (equation 6.17):



The oxidation reactions can take place within a very short time of exposure and considering that calcine water comes with high iron concentrations (Table 2.2), ferrous and ferric ions are ubiquitous on the pyrite surface and in solution. Examination of speciation diagrams for both ferrous and ferric ions (Figures 2.32 and 2.33) shows that at the plant flotation pH of 7.2, all the ferric iron is present as ferric hydroxide ($\text{Fe}(\text{OH})_3$) while approximately 70% of ferrous iron is in complex form (FeOH^+) and 30% is available as Fe^{2+} . The

effect of iron ions on pyrite flotation with SIBX is therefore dependant on interaction between SIBX and each of the three species.

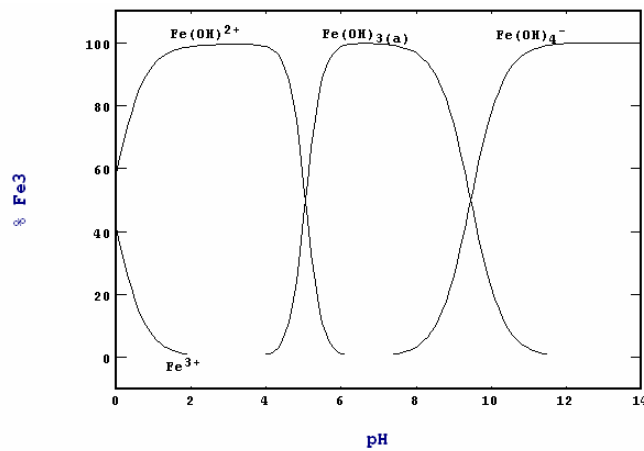


Figure 2.32 Speciation diagram for $2 \times 10^{-3}M$ Fe(III) as a function of pH at 25°C. STABCAL Software, NBS Database

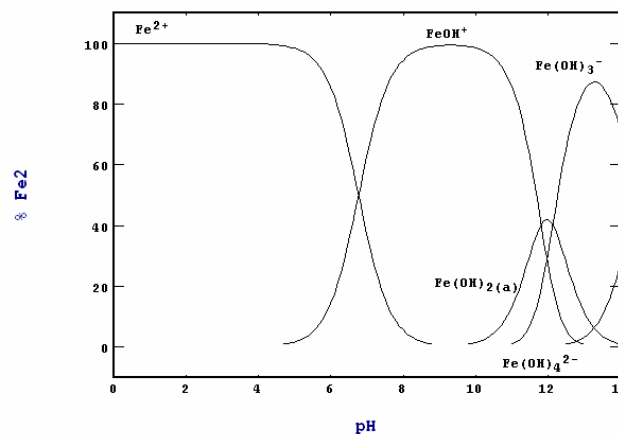


Figure 2.33 Speciation diagram for $2 \times 10^{-3}M$ Fe(II) as a function of pH at 25°C. STABCAL Software, NBS Database

Jiang and co-workers (1998) have investigated the effect of ferric and ferrous ions on the flotation behaviour of ore-pyrite as a function of pH. While xanthate alone gave complete flotation in acidic and alkaline regions, the presence of ferric ions gave partial flotation in the intermediate pH range (Figure 2.34). This is the region in which ferric hydroxide is stable (Figure 2.32). By using distribution diagrams of the iron-xanthate-water system, the authors were able to show that a weakly hydrophobic and insoluble ferric

dihydroxy xanthate complex ($\text{Fe}(\text{OH})\text{X}_2$) is formed. The sequence of reagent addition and pH adjustment was found to have a remarkable effect on pyrite flotation response in the neutral pH region. In the presence of ferric ions, adjustment of solution pH before addition of xanthate gave more significant depression that the reverse-order. This is important as it predicts the behaviour of ferric ions released into solution by a low pH treatment aimed at “polishing” oxidised pyrite prior to flotation.

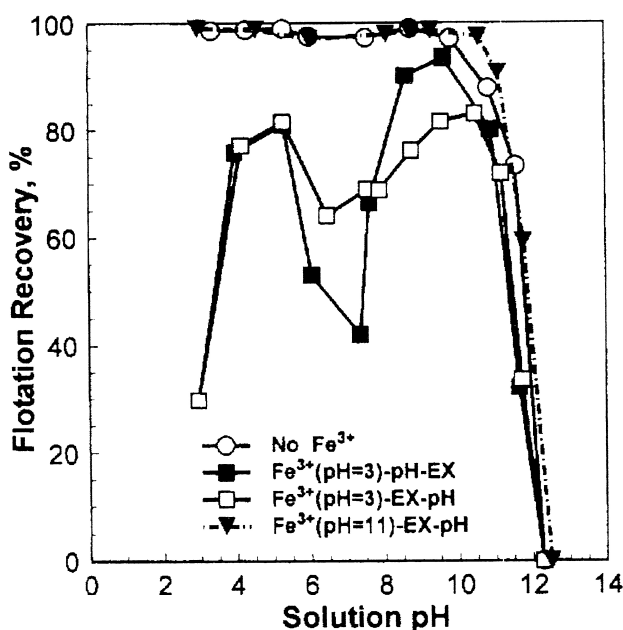


Figure 2.34 Effect of pH and reagent addition order on the flotation of ore-pyrite in the absence and presence of $2 \times 10^{-3} \text{M}$ Fe^{3+} ions using $3.3 \times 10^{-4} \text{M}$ ethyl xanthate (EX) and 50mg l^{-1} MIBC. Conditioning time and reagent addition order: (■) Fe^{3+} (2 min) at pH 3 → pH adjustment (2 min) → EX (2 min); (□) Fe^{3+} (2 min) at pH 3 → EX (2 min) → pH adjustment (2 min); (▼) Fe^{3+} (2 min) at pH 11 → EX (2 min) → pH adjustment (2 min) (Jiang et al., 1998)

In Figure 2.35, ferrous ions too were shown to significantly affect pyrite flotation in neutral to weakly alkaline solutions. The authors observed that in the presence of ferrous ions, complete flotation was observed below about pH 5-6 irrespective of reagent addition order. This behaviour was attributed to the solubility of ferrous xanthate being high in acidic pH so that no significant

side-reactions between ferrous and xanthate ions occurred during flotation. The drastic decrease in pyrite flotation at about pH 6 was attributed to reactions between ferrous iron with xanthate to form a weakly hydrophobic compound on pyrite and in the solution. The authors assumed this to be ferric di-hydroxy xanthate.

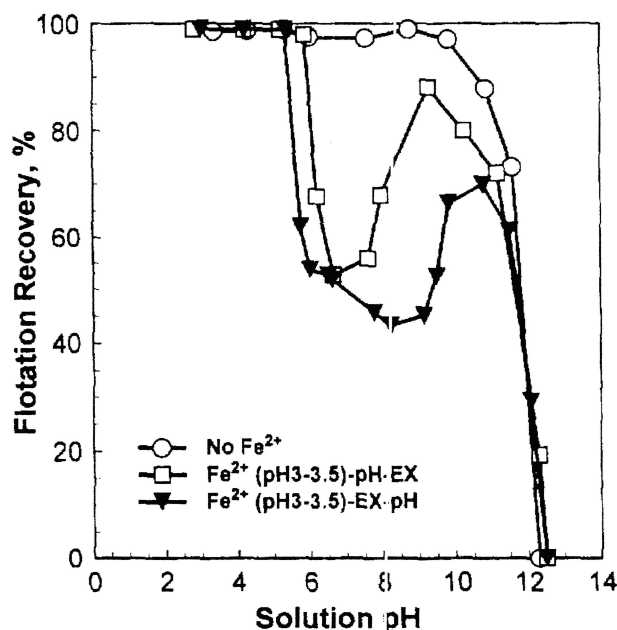


Figure 2.35 Effect of pH and reagent addition order on the flotation of ore-pyrite in the absence and presence of $2 \times 10^{-3} \text{M}$ Fe^{2+} ions using $3.3 \times 10^{-4} \text{M}$ ethyl xanthate (EX) and 50mg l^{-1} MIBC. Conditioning time and reagent addition order: (\square) Fe^{3+} (2 min) at pH 3.0-3.5 \rightarrow pH adjustment \rightarrow EX (2 min); (\blacktriangledown) Fe^{2+} (2 min) at pH 3.0-3.5 \rightarrow EX (2 min) \rightarrow pH adjustment (2 min) (after Jiang et al., 1998)

2.6.5 Iron Ions and Surface Charge

The oxidation products formed on the surface such as ferrous ions, and the hydroxyl complexes produced after the addition of caustic to neutralise pH also play an important role in influencing surface electrical properties and hence, floatation of pyrite with xanthate. As highlighted by Fuerstenau (1982c), when the inorganic species are adsorbed on the surface, they affect the sign and magnitude of surface charge, thereby controlling the adsorption

of physically adsorbing flotation agents. Once a surface charge exists, other ions from the bulk solution must be adsorbed as counter-ions for electro-neutrality. This gives rise to an electrical double layer. In a system involving pyrite and its oxidation products, hydrogen and hydroxyl ions are free to pass between the solid phase and the liquid phase and are therefore called potential determining ions. The activity of these ions at which surface charge is zero is called the point of zero charge (PZC). The importance of this parameter is that the sign of surface charge has a major effect on the adsorption of all other ions and particularly those charged oppositely to the surface because they function as counter ions to maintain electro-neutrality.

Jiang et al. (1998) have showed that at a modest degree of oxidation; pyrite surfaces behave like iron oxide with a PZC at pH 7. This is due to the presence of ferric hydroxide formed during oxidation. The surface will acquire electro-kinetic features of the iron hydroxide. The authors showed that in the presence of 2×10^{-3} M ferric ions and 5.6×10^{-4} M ethyl xanthate, the zeta potential of pyrite exhibited less positive charge below pH 7.5 compared with that in the presence of ferric xanthate alone. At pH > 7.5, there was no noticeable difference between the two. This implies that in the presence of ferric ions, adsorption of xanthate onto pyrite is favoured in acidic conditions only.

Jiang and co-workers also showed that the PZC of pyrite in the presence of 2×10^{-3} M ferrous ions is pH 9. Addition of 5.6×10^{-4} M ethyl xanthate reduced it to pH 6. The authors observed that at pH < 6, the zeta potential curve was identical to that in the presence of xanthate only and at pH > 6, it was identical to that in the presence of only ferrous ions. From these results, they concluded that ferrous ions do not undergo significant reaction with xanthate at pH < 6 and the flotation of pyrite in this region is mainly due to the adsorption of xanthate on the surface. At pH > 6, the adsorption of xanthate was reduced, which was in agreement with their flotation results.
